

IMPROVED BRAKING PERFORMANCE OF AN ELECTRIC VEHICLE BY INTEGRATING PLUG BRAKING WITH REGENERATIVE BRAKING

AMRIT ANAND MAHAPATRA



**DEPARTMENT OF ELECTRICAL ENGINEERING
NATIONAL INSTITUTE OF TECHNOLOGY
ROURKELA - 769008
JANUARY 2015**

IMPROVED BRAKING PERFORMANCE OF AN ELECTRIC VEHICLE BY INTEGRATING PLUG BRAKING WITH REGENERATIVE BRAKING

A thesis submitted for the partial fulfilment of the requirements for the
award of the degree of
**MASTER OF TECHNOLOGY BY RESEARCH
IN
ELECTRICAL ENGINEERING**

BY
AMRIT ANAND MAHAPATRA

UNDER THE GUIDANCE OF
DR. S. GOPALAKRISHNA



**DEPARTMENT OF ELECTRICAL ENGINEERING
NATIONAL INSTITUTE OF TECHNOLOGY
ROURKELA - 769008
2012 - 2014**

*Improved Braking Performance of an Electric
Vehicle by Integrating Plug Braking with
Regenerative Braking*

Amrit Anand Mahapatra

Dedicated
To my revered Grand-Parents &
To my loving Parents



DEPARTMENT OF ELECTRICAL ENGINEERING
NATIONAL INSTITUTE OF TECHNOLOGY
ROURKELA
ODISHA - 769008

CERTIFICATE

This is to certify that the research thesis entitled “**Improved Braking Performance of an Electric Vehicle by Integrating Plug Braking with Regenerative Braking**” by **Amrit Anand Mahapatra** submitted to **National Institute of Technology, Rourkela** for the award of Master of Technology by Research in Electrical Engineering is a record of bona fide research work carried out by him in the Department of Electrical Engineering under my supervision. I believe that this thesis fulfils part of the requirements for the award of degree of **Master of Technology by Research in Electrical Engineering**. The results embodied in the thesis have not been submitted for the award of any other degree elsewhere.

Place: Rourkela

Date:

Dr. S. Gopalakrishna
Research Guide
Department of Electrical Engineering
NIT Rourkela

ACKNOWLEDGEMENT

Every successful research work requires a bounty amount of patience, a supreme guidance and an assistance and assurance of many people. I express my sincere thanks and deep sense of revered and heartily gratitude to my supervisor Dr. S. Gopalakrishna for his excellence guidance and unwavering inspiration. It's because of his tremendous support, dedication and inspiration, the thesis has achieved this context. I will always cherish these days of work with immense sense of respect and pleasure.

I am highly indebted to Prof. A. K. Panda, HOD, Department of Electrical Engineering, National Institute of Technology, Rourkela for providing me with all the necessary facilities. I also thank Prof. S. Ganguly (Faculty, Department of Electrical Engineering) and Prof. P. M. Khillar (Faculty, Department of Computer Science) who guided me necessarily as the members of the Masters Scrutiny Committee. I am highly obliged to Dr. S. Samanta, Dr. S. Maity and Dr. M. Pattnaik of Department of Electrical Engineering for their valuable suggestions in the due course of research. I also express my deep sense of gratitude to all the faculty members and staff of the Department of Electrical Engineering for giving me the timely support as and when required. I am thankful to and fortunate enough to get constant encouragement from all my friends and senior research scholars. I would like to extend my heartily thanks to Soumya, Gourishankar, Pradosh Sir, Sushant Sir, Subhashis Sir, Amit Sir, Pragyan Madam, Bijayini Madam and Deepika for their constant moral boosting throughout this research work.

I owe my profound gratitude to all my family members. The heavenly blessing of my grandfather and the spirited love of my grandmother has brought laurels to my work. With high sense of respect and reverence, I owe my heartily thanks to my parents for their constant support and encouragement. I bow with my folded hands to The Almighty for enlightening the path in my ignorance and for holding me during the entire period of ups and downs to fight back in research work with a firm determination. I would apologize if I failed to acknowledge anyone.

Amrit Anand Mahapatra

ABSTRACT

With the increase in demand for green energy, new technologies are evolved to improve energy efficiency. One of the methods to improve energy efficiency in electric vehicles and hybrid electric vehicles is regenerative braking. As regeneration is not effective during low speeds, hydraulic braking is being used along with regenerative braking. Different control algorithms are proposed in literature for proper selection between the two types of braking. The hydraulic braking system consists of multiple pistons that provide equal distribution of braking force on the wheels. However, this can be directly achieved by providing necessary braking torque on the shaft by applying dissipative braking at low speeds using an auxiliary motor parallel to the traction motor. In this thesis, a method is proposed where two induction motors are used, one as the traction motor and other as an auxiliary motor to demonstrate braking phenomenon. Plug braking of auxiliary motor is integrated with regenerative braking of main motor by coupling both the shafts of the two motors. The advantage of this method is that force is directly acting on the shaft and hence equal braking force is distributed on all the wheels, even at low speeds. The auxiliary motor can also be used for propulsion according to the torque demand and peak regeneration current can be counteracted by the plugging current thus limiting the battery current to its range. The disadvantage is that some amount energy is dissipated during plugging for small duration at low speeds. A transient analysis implementing vector control of induction machine is performed in Matlab and the results show good braking performance.

Keywords: - Electric Vehicles, Induction Machine, Battery, Plug braking, Regenerative braking, Main Motor, Auxiliary Motor, Field Oriented Control

TABLE OF CONTENTS

I. ACKNOWLEDGEMENT	i
II. ABSTRACT	ii
III. TABLE OF CONTENTS	iii
IV. LIST OF FIGURES	v
V. LIST OF ABBREVIATIONS	vii
VI. LIST OF TABLES	ix

CHAPTER 1

INTRODUCTION

1.1 Overview	2
1.2 Research Background	2
1.3 Motivation	5
1.4 Objective of Research	6
1.5 Thesis Organisation	7

CHAPTER 2

MATHEMATICAL MODELING OF VEHICLE, INDUCTION MACHINE AND BATTERY

2.1 Introduction	9
2.2 Vehicle Model	13
2.3 Induction Machine Model	17
2.3.1 Steady State Operation of Induction Machine	17
2.3.2 Dynamic Modeling of Induction Machine	19
2.4 Battery Model	26
2.5 Summary	29

CHAPTER 3

BRAKING ANALYSIS OF AN ELECTRIC VEHICLE WITH INDUCTION MOTOR DRIVE

3.1 Introduction	31
3.2 Plug Braking Analysis of IM	31

3.2.1 Voltage Oriented Control	31
3.2.2 Results and Discussion	32
3.3 Regenerative Braking Analysis of IM	35
3.3.1 Field Oriented Control	35
3.3.2 Voltage Source Based Current Control	40
3.3.3 Results and Discussion	44
3.4 Summary	47
CHAPTER 4	
BRAKING ANALYSIS BY INTEGRATING PLUG BRAKING WITH REGENERATIVE BRAKING	
4.1 Introduction	49
4.2 Hybrid Electrical Braking System	49
4.3 Results and Discussion	50
4.4 Summary	54
CHAPTER 5	
CONCLUSION AND SCOPE FOR FUTURE WORK	
5.1 Conclusion	56
5.2 Scope for Future Work	56
APPENDIX 1	57
APPENDIX 2	59
APPENDIX 3	61
APPENDIX 4	63
APPENDIX 5	66
REFERENCES	67
THESIS DISSEMINATION	71
BIO-SKETCH	72

LIST OF FIGURES

1.	Fig. 2.1.	Power flow illustration of hybrid drive train	9
2.	Fig. 2.2.	Characteristic of traction system	10
3.	Fig. 2.3.	Torque Speed Characteristics of DC Motor	11
4.	Fig. 2.4.	Torque Speed Characteristics of Induction Motor	11
5.	Fig. 2.5.	Torque Speed Characteristics of PMSM Motor	12
6.	Fig. 2.6.	Torque Speed Characteristics of SRM Motor	12
7.	Fig. 2.7.	Lateral force components on the vehicle	13
8.	Fig. 2.8.	Drive line model of vehicle	15
9.	Fig. 2.9.	Power slip characteristics of induction machine	17
10.	Fig. 2.10.	Torque slip characteristics of induction machine	18
11.	Fig. 2.11.	Modes of operation in induction machine	18
12.	Fig. 2.12.	Three phase stationary reference frame	19
13.	Fig. 2.13.	Two phase stationary reference frame	22
14.	Fig. 2.14.	Synchronously rotating reference frame	22
15.	Fig. 2.15.	Dynamic or d-q equivalent circuit of induction machine	23
16.	Fig. 2.16.	Comparison of rotor speed with RMF speed	25
17.	Fig. 2.17.	Variation of torque with speed	26
18.	Fig. 2.18.	Nonlinear battery model	27
19.	Fig. 2.19.	Equivalent block diagram of Li-Ion battery model	28
20.	Fig. 3.1.	Dynamic model of induction machine using VOC	31
21.	Fig. 3.2.	Variation of speed during plug braking	33
22.	Fig. 3.3.	Variation of torque during plug braking	33
23.	Fig. 3.4.	Variation of battery voltage during plug braking	33
24.	Fig. 3.5.	Variation of battery current during plug braking	34
25.	Fig. 3.6.	Variation of SOC during plug braking	34
26.	Fig. 3.7.	Torque production in a current loop	36
27.	Fig. 3.8.	Dynamic model of induction machine with FOC	37
28.	Fig. 3.9.	Field oriented control of induction machine	38
29.	Fig. 3.10.	Speed and torque control	39
30.	Fig. 3.11.	Field oriented control of induction machine model	39
31.	Fig. 3.12.	Voltage source based current controller	42

32.	Fig. 3.13.	Variation of machine speed with regenerative braking	44
33.	Fig. 3.14.	Variation of RMF speed with regenerative braking	45
34.	Fig. 3.15.	Variation of machine torque with regenerative braking	45
35.	Fig. 3.16.	Variation of battery voltage with regenerative braking	45
36.	Fig. 3.17.	Variation of battery current with regenerative braking	46
37.	Fig. 3.18.	Variation of power with regenerative braking	46
38.	Fig. 3.19.	Variation of SOC of battery with regenerative braking	46
39.	Fig. 4.1.	Block diagram of hybrid electrical braking system	49
40.	Fig. 4.2.	Variation of vehicle speed with hybrid braking system	52
41.	Fig. 4.3.	Variation of torque with hybrid braking system	52
42.	Fig. 4.4.	Variation of battery voltage with hybrid braking system	52
43.	Fig. 4.5.	Variation of battery current with hybrid braking system	53
44.	Fig. 4.6.	Variation of power with hybrid braking system	53
45.	Fig. 4.7.	Variation of SOC of battery with hybrid braking system	53
46.	Fig. A1.1.	Block diagram of series HEV	57
47.	Fig. A1.2.	Block diagram of parallel HEV	57
48.	Fig. A1.3.	Block diagram of series-parallel HEV	57
49.	Fig. A1.4.	Power flow during starting of the vehicle	58
50.	Fig. A1.5.	Power flow during cruising of the vehicle	58
51.	Fig. A1.6.	Power flow during braking of the vehicle	58
52.	Fig. A5.	Flowchart for Simulation Study of Improved Braking Analysis	66

LIST OF ABBREVIATIONS

d	:	direct axis
q	:	quadrature axis
s	:	stator variables
r	:	rotor variables
F_{ij}	:	flux linkage variables ($i = q$ or d and $j = s$ or r)
F_{mq}, F_{md}	:	q and d axis magnetizing flux linkage variables
v_{qs}, v_{ds}	:	q and d axis stator voltages
v_{qr}, v_{dr}	:	q and d axis rotor voltages
i_{qs}, i_{ds}	:	q and d axis stator currents
i_{qr}, i_{dr}	:	q and d axis rotor currents
R_r	:	rotor resistance
R_s	:	stator resistance
X_{lr}	:	rotor leakage reactance
X_{ls}	:	stator leakage reactance
L_s	:	stator inductance
L_r	:	rotor inductance
L_m	:	mutual inductance
P	:	number of poles
J	:	moment of inertia
T_e	:	electrical output torque
T_L	:	load torque
ω_e	:	stator angular electrical speed
ω_b	:	motor angular base electrical speed
ω_m	:	rotor angular electrical speed
V_{batt}	:	Battery Voltage
E_0	:	Battery Constant Voltage
K	:	Polarization Constant or Polarization Resistance
Q	:	Battery Capacity
it	:	$\int idt =$ Actual Battery Charge
A	:	Exponential Zone Amplitude

B	:	Exponential Zone Time Constant Inverse
R	:	Internal Resistance
$i(t)$:	Battery Current
i^*	:	Filtered Current
F_{acclr}	:	force used for acceleration
F_x	:	force due to traction
F_{aero}	:	aerodynamic drag force
F_{roll}	:	rolling resistance force
$F_{gravity}$:	gravitational force
V_x	:	vehicle velocity in the x – direction
m_v	:	mass of the vehicle along with passenger load
g	:	gravitational acceleration
α	:	angle of inclination of the road
s_x	:	the normalized slip
r_w	:	dynamic rolling radius of wheel
ω_w	:	angular speed of wheel
μ_{s0}	:	longitudinal friction coefficient
ρ	:	mass density of air
C_d	:	aerodynamic drag coefficient
A_f	:	frontal area of the vehicle
V_{wind}	:	wind velocity
f_r	:	coefficient of rolling resistance
η_{dr}	:	driveline efficiency
g_{dr}	:	gear ratio
ω_r	:	shaft speed
ω_b	:	base speed

LIST OF TABLES

1. Table I	Vehicle Parameters	59
2. Table II	Machine Parameters of 50-hp Induction Motor	59
3. Table III	Machine Parameters of 3-hp Induction Motor	60

CHAPTER 1

INTRODUCTION

OVERVIEW

RESEARCH BACKGROUND

MOTIVATION

OBJECTIVE OF RESEARCH

THESIS ORGANISATION

1.1 OVERVIEW

Electric Vehicles (EVs) and Hybrid Electric Vehicles (HEVs) are smart alternatives to traditional vehicles driven by internal combustion engines (ICEs) in the era of green technology. They improve the fuel economy of the automobile industry. However the high cost of EVs/HEVs has put them off the road in a wide scale. The expensiveness of EVs/HEVs is due to the complexity of bidirectional power-flow. Hence, research and development is focused to simplify the EV configuration so as to make it more user friendly. One of the major area of research aims to develop strategies in order to increase the regeneration of power being wasted during braking. In this thesis, the braking problem has been analyzed and an algorithm has been proposed to improve the overall performance of the vehicle during braking.

1.2 RESEARCH BACKGROUND

Automobiles play an important role in the life of modern society. An automobile with internal combustion engine (ICE) is a significant achievement of the modern technology which has earned laurels in the industry. However the gigantic development of the automobile industry across the globe is a serious threat to the environment and fossil fuel resources [1]. Therefore, the present research in the automotive industry is focused to design the electric transportation system for providing clean, secure and smart alternative in the form of EVs and HEVs. EVs have their own advantages as well as challenges. Considering the electricity being generated from fossil fuels, EVs prove to be more efficient in comparison to ICE vehicles in terms of both equivalent miles and the cost of driving per mile. The electricity is also generated from renewable resources which provide the minimal threatening to pollution and resources [2]. However the high cost, limited driving range and long charging time have handicapped battery driven vehicles, thereby paving the way for HEVs in which the drive train depends both on the conventional ICE and electrical machines. This can overcome the issue of cost and driving range of pure EVs without requiring to be plugged in for charging. The fuel consumption in HEVs is significantly decreased in contrast to conventional vehicles [3-5].

Although the preliminary design of EVs/HEVs was done few decades back, improvements are being done in recent years to reduce the cost, increase the energy efficiency, choose a proper traction motor etc. Proper modelling of essential components of the vehicles like battery and traction motor as well as vehicle load (load to the traction motor) are essential requirement for simulation of electrical characteristics. Simulation studies are being performed

by using various numerical methods. Advanced techniques like Finite Element Analysis (FEA) are also being used for effective modeling. A mathematical model of a vehicle load is obtained by considering different forces acting on the vehicle. The dynamics of the vehicle movement mathematically describe the vehicle behavior based on the principles of mechanics. These vehicle dynamics determine the ideal torque-speed profile for the traction system [5, 6]. The traction motor is selected on the basis of traction requirement of the vehicle and driving road characteristics. A comparative study has been outlined by the authors [7, 8] for the various types of electric motor drive systems in accordance with the vehicle propulsion system. Considering the power-density, traction requirements, efficiency, maintenance and expenses, reliability and maturity of use, the induction motor drive (IM) emerges as a potential workhorse for electrical traction machine in EVs/HEVs, in its race with a DC motor drive, switched reluctance motor drive (SRM) and synchronous motor/permanent magnet brushless motor drive (PMSM/ BLDC).

Generally, a three phase induction machine (3Φ IM) is used in the EVs or HEVs. However the analysis during dynamic conditions of the 3Φ IM is mathematically complicated. Hence the method of linear transformation of variables is included in the study through which the variables in the 3Φ system were transformed into equivalent model of IM in the synchronously rotating reference frame while retaining the steady state and dynamic performance of the machine with the criteria of invariance of power [11-16].

The electrical energy source in EVs and HEVs is generally a rechargeable battery. The various models of the battery have been analyzed in [17] considering the nonlinear characteristic of the battery with respect to the state of charge (SOC) of the battery. The two major types of battery models are 1) Circuit Oriented Battery Models and 2) Mathematical Battery Models. A simple review of the various models of the battery depicting its non-linear characteristic is analyzed in [18]. The steady state characteristics and the performance of the battery were analyzed and compared using the traditional mathematical model as well as the circuit oriented equivalent battery models. In reference [19], the authors have developed a battery model in application to dynamic simulation software using SOC as the state variable. This battery model has been included in SimPowerSystems simulation software and is used in the demo of HEV in MATLAB/Simulink. The four major types of batteries i.e. Lead Acid, Lithium Ion (Li - Ion), Nickel Cadmium (Ni - Cd), Nickel Metal Hydride (Ni - MH) are analyzed so as to extract the parameters from the discharge curves. The dynamic models of the major types of batteries available for application in EVs are analyzed and validated in [20].

The state space equations for the charging and discharging characteristics as well as the SOC for the major types of chemical batteries have been derived in [20-22].

Braking is an essential feature of almost all the electrical drives. The braking performance is the first concern in the design of any vehicle dynamic system. An efficiently designed braking system for a vehicle must always meet the distinct demand of quickly reducing the vehicle speed and maintaining the vehicle direction [1]. In traditional vehicles driven by ICEs, hydraulic braking is the only mean of effective braking. The hydraulic brake system is quite essential for the proper realization of the vehicle dynamics [23]. The hydraulic braking is the process in which brake pad is pressed to brake plate which develops a braking force on the tire ground contact area. Anti-lock brake system (ABS) is an established method of braking in automobiles because of its superiority in terms of safety requirements [24]. For a vehicle travelling in the stop and go pattern of urban traffic a huge amount of kinetic energy goes waste in the process of braking. However, there is no scope of restoring back the energy being wasted in the braking process.

With the advent of EVs and HEVs, electrical braking has gained a lot of importance in terms of its effectiveness. Basically the methods of electrical braking include regenerative braking, plug braking and dissipative braking. But regenerative braking and plug braking are widely used because the former is known for its braking energy efficiency and the latter is known for its braking time efficiency [25-28]. Plug braking can be obtained by reversing the phase of any two terminals out of the 3Φ supply terminals of the IM. With the reversal of terminals, the torque also reverses which opposes the normal operation of the machine and reduces the speed of the vehicle and thus braking is obtained. The regenerative braking is obtained by driving the rotor with a negative slip. With the slip being negative, the machine operates as a generator and the load supplies power to the source, thereby the direction of current and torque reverses which causes braking in the drive. However, the hydraulic brake unit is always kept as a reserve brake unit for situations when the electric brake system is limited by the power rating of the motor, speed of the vehicle and the state of charge of the battery [29]. Thus to have a proper coordination between the electric brake system and the frictional brake system, various control strategies which can be either series or parallel are developed. This coordinated control is called as hybrid brake system. An efficient hybrid braking system should consider (1) sufficient braking force to quickly reduce speed, (2) maximum regeneration of the braking energy and (3) proper braking force distribution on the wheels to ensure vehicle stability during braking [1].

The present hybrid system of braking is a combination of hydraulic braking and regenerative braking. In this system an electric motor is used for the purpose of braking. The desired braking can be obtained through a parallel brake system implementing regenerative braking and hydraulic braking simultaneously [31]. In [32] ABS is introduced with regenerative braking where a DC motor is connected to the wheels through reduction gears. Although the regenerative approach to hydraulic brake system increases the efficiency, but the use of additional components like sensors, transducers and controllers makes the system more complex [31 - 37].

The method of hybrid braking system is a hybridization of mechanical and electrical system. This method of hybridization facilitates mechanical interactions, which improves the torque and speed requirement of the vehicle. But there is no electrical interaction with this system, hence the battery performance is not so improved. In order to improve the hybrid braking system, the hydraulic braking can be substituted by plug braking by the use of an auxiliary motor. The main motor drives the traction system and is also used for regenerative braking. This method of electrical braking has been discussed in this research work and the advantages and disadvantages have been outlined.

1.3 MOTIVATION

Although mechanical braking is a reliable braking method being used since the advent of vehicles, it dissipates the kinetic energy of the wheels. Electrical braking is an effective method which can be implemented along with the hydraulic braking for stop and go drive strategy in busy traffic. Plug braking and regenerative braking are two important methods of braking employed by the use of electric traction motor in EVs/HEVs. The method of plugging is efficient enough in terms of its fastness, but there was no regeneration of the kinetic energy into the battery during the process of braking. There in the concept of regenerative braking was evoked. During the process of regenerative braking, power is adaptively restored into the battery which improves the overall energy efficiency. But regenerative braking cannot produce sufficient braking force as desired by the driver due its limitations [23].

The present hybrid braking system is a combination of regenerative braking and hydraulic braking where the latter is put into action beyond the limitations of electrical braking. Regenerative braking is limited by maximum power of the motor, the SOC of the battery and the vehicle speed. The motivation here is to develop a hybrid braking method which uses two IMs connected in parallel. One motor is of power rating equivalent to the traction system of

the vehicle and is used as the main propulsion drive motor. This motor operates in the regenerating mode for the purpose of braking. The other motor is of lower power rating and operates in plugging mode as when fast braking is desired. The combined effect of main motor and auxiliary motor produces sufficient braking torque required for the effective retardation of the vehicle.

The drive-line topology of EVs and HEVs is quite complex because of the integration of various circuits within it. The EV usually consists of an electric motor, power electronic converter, battery, electric control unit, brake management unit, transducers and sensors. Voltages are converted from DC to 3 Φ AC between the battery and IM. A thorough analysis of the entire system is quite complex and time consuming. A simplified analysis of IM is carried out using dynamic equivalent circuit of a 3 Φ IM, where input sinusoidal voltages and currents are transformed to dc quantities. The dynamic modeling of the 3 Φ IM allows the direct interfacing with the battery without the use of any power electronic devices.

1.4 OBJECTIVE OF RESEARCH

Braking forms an important aspect of any on-road vehicle. For the widespread development of EVs and HEVs, developing an efficient braking method is one of the major research areas.

The research objective focusses

- To develop a DC equivalent model of the motor and battery system excluding the conversions with the use of proper transformations.
- To develop a logic to implement proper sharing of kinetic energy of the wheel between plugging (using auxiliary motor) and regeneration (using main motor).
- To implement plug braking at lower speeds effectively where the method of regenerative braking fails.

1.5 THESIS ORGANISATION

CHAPTER 1 gives an introductory preface to the thesis. The research background of the thesis is presented which motivated the author towards the research objective in the field of braking analysis of induction machines in applications to EVs or HEVs.

In CHAPTER 2 the longitudinal dynamics governing the acceleration of the vehicle are discussed. From the vehicle dynamics the traction characteristics of the vehicle are introduced. Based on this traction characteristics, the torque speed characteristics of the various electrical machines suitable for the traction drive are discussed. The characteristics of the induction machine and the power flow during the various modes of operations are studied. The dynamic modeling of the induction machine and battery is analyzed.

In CHAPTER 3 the analysis of plug braking and regenerative braking are discussed with applications to electric vehicles. The battery model is interfaced with the dynamic model of IM. To simplify the analysis of the model, voltage oriented control and field oriented control have been used. The advantages and disadvantages of plug braking and regenerative braking are discussed.

In CHAPTER 4, the integration of plug braking with regenerative braking operation is considered. Both the types of braking have been implemented through two Induction Machines of different ratings to drive the same traction system which improves the overall efficiency of the machine as well as improves the effectiveness of braking in electric vehicles.

In CHAPTER 5 the overall conclusion of the thesis has been briefed. Here also a short note about the scope of extending the current work has been texted.

CHAPTER 2
MATHEMATICAL MODELING OF VEHICLE,
INDUCTION MACHINE AND BATTERY

INTRODUCTION
VEHICLE MODEL
INDUCTION MACHINE MODEL
BATTERY MODEL
SUMMARY

2.1 INTRODUCTION

Electric Vehicles (EVs) employ an electric motor for the traction purpose and chemical batteries as energy sources. Hybrid Electric Vehicles (HEVs) include the advantages of both EVs and the traditional vehicles. Since HEVs employ two power trains, the driving and the braking system become complicated. Usually a bidirectional power train is employed for the purpose of recapturing the braking energy [1] as shown in Fig. 2.1. The two power sources for propulsion in EVs/HEVs can be connected in series or parallel according to the power flow. According to the methods of connection of the power sources the topologies of HEV can be basically classified [5] into 1) Series HEV 2) Parallel HEV and 3) Series Parallel HEV shown in Fig. A1.1 to Fig. A1.3 of Appendix 1. The power flow during the various modes of operation of the vehicle are shown in Fig. A1.4 to Fig. A1.6 of Appendix 1.

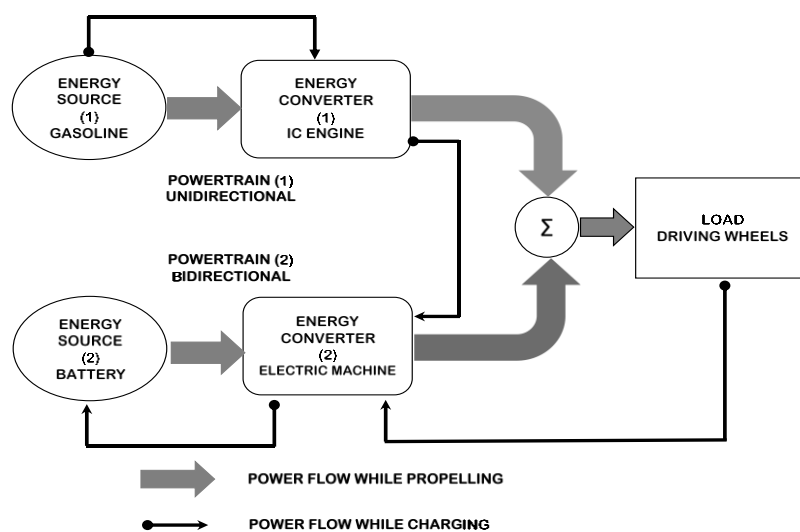


Fig. 2.1. Power flow illustration of hybrid drive train [1]

A well designed electric traction system should satisfy the following requirements [1]

- 1) A high instant power and a high power density
- 2) A high torque at low speeds for starting and climbing, as well as a high power at high speed for cruising
- 3) A very wide speed range, including constant-torque and constant-power regions
- 4) A fast torque response
- 5) A high efficiency over the wide speed and torque ranges

- 6) A high efficiency for regenerative braking
- 7) A high reliability and robustness for various vehicle operating conditions
- 8) A reasonable cost

The electrical machines employed in the EVs and HEVs should have characteristics similar to that of the traction characteristics of vehicle dynamics. The machine usually requires

- Frequent start and stops
- High rates of acceleration/deceleration
- Very wide speed range of operation
- High torque and low speed (hill climbing operation)
- High speed and low torque (cruising operation)

Considering all the factors for traction purpose discussed above, the most suitable electric machines for the purpose of electric propulsion system are listed as

- Direct Current (DC) Motors
- Induction Motors (IM)
- Permanent Magnet Synchronous Motors (PMSM)
- Switched Reluctance Motors (SRM)

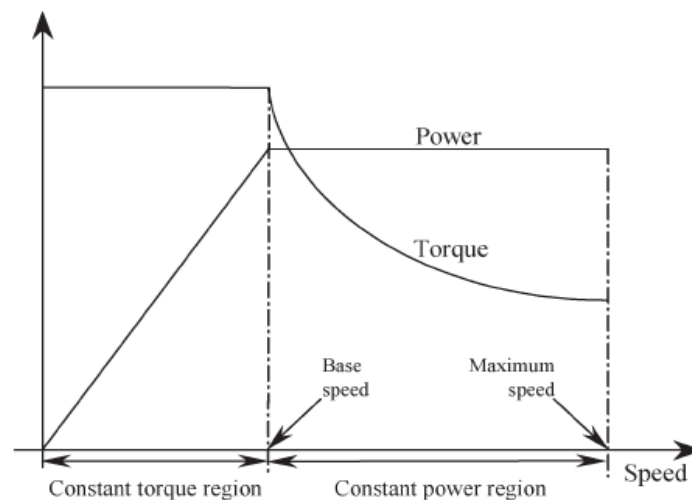


Fig. 2.2. Characteristic of traction system

The torque-speed characteristics of the various motors used for the traction purpose are shown in Fig. 2.3. to Fig 2.6. for DC machine, induction machine, PMS machine and SR machine respectively.

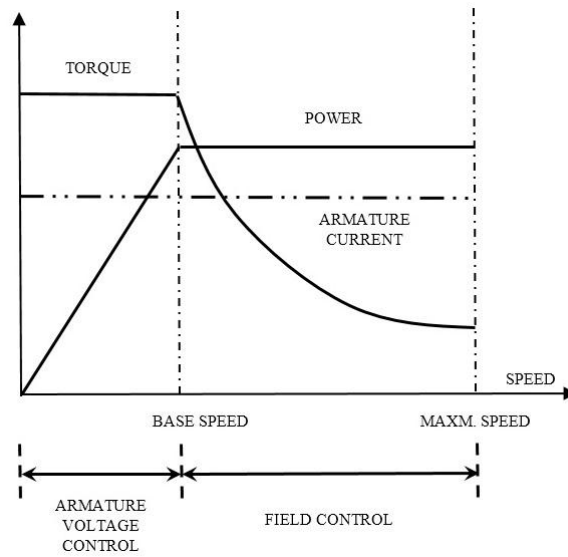


Fig. 2.3. Torque Speed Characteristics of DC Motor

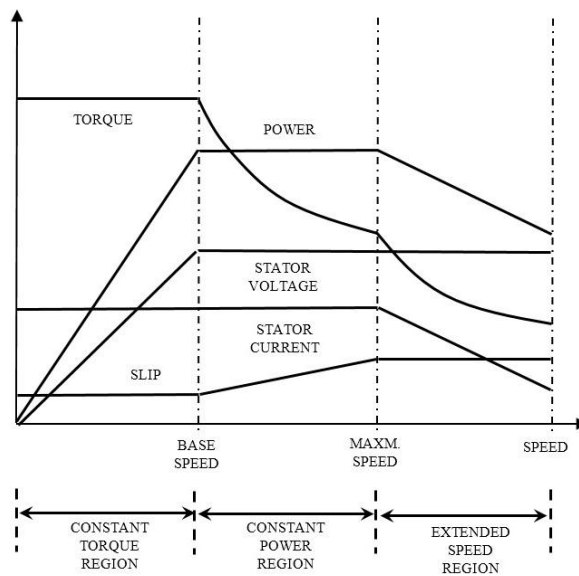


Fig. 2.4. Torque Speed Characteristics of Induction Motor

Comparing these torque speed characteristics with traction characteristics shown in Fig. 2.2, we can conclude that DC machine has the best performance for the traction purpose as its torque-speed characteristics are quite similar to the traction characteristics corresponding to vehicle dynamics. However its disadvantages like bulky construction, low reliability, low ruggedness and need of high maintenance due to the use of commutator gave the way for AC induction motors and synchronous motors. The permanent magnet synchronous motor (PMSM) are well suited for EVs as they have a high torque density, reduced weight and volume and high efficiency. The power to weight ratio of synchronous motor is appreciably good in

comparison to that of IM. However they have a short constant power region of operation as compared to IM due to their limited field weakening capability which also limits the speed of operation.

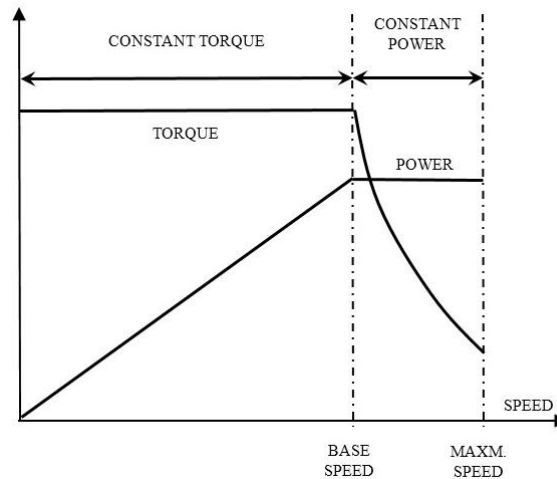


Fig. 2.5. Torque Speed Characteristics of PMSM Motor

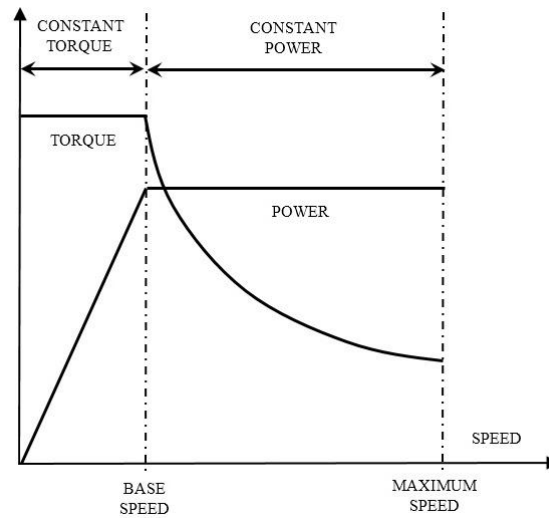


Fig. 2.6. Torque Speed Characteristics of SRM Motor

The magnetic material used for PM machines is neodymium-iron-boron (NdFeB). There has been a sharp increase of this material to around 150 US\$/kg due to virtual market monopoly. This is also a rare earth material which is in the verge of depletion for extensive future use [47] [48]. Switched reluctance motors (SRM) are gaining importance because of its simple as well as rugged construction and high speed operation. But the drawbacks of high torque ripple and acoustic noise making the motor unacceptable for vehicular applications.

Out of the various available electrical machines suitable for traction system in EVs/HEVs, the Induction Machine (IM) is selected as one of the best performer for the traction purpose as its torque speed characteristic is quite similar to the traction requirement. Moreover, dynamic modeling of the 3Φ IM into its equivalent dq model in synchronous frame simplifies the mathematical complexity. Extended speed range of operation with constant power beyond the base speed is accomplished by flux weakening. The major source of supply in EVs/HEVs is the battery which acts as a source of power during normal propulsion and sink of power during regenerative braking. In this chapter, a mathematical model of the vehicle load at the shaft of the traction motor is presented. The dynamic modeling of the IM is also discussed so as to simplify the braking analysis of IM in application to EVs and HEVs. Finally a simple analysis of the lithium ion battery using the mathematical modeling is performed.

2.2 VEHICLE MODEL

The load to the traction motor [38] is the resistance offered to the movement of the vehicle. A vehicle whose parameters are listed in Table I in Appendix 2 taken from [6] is considered for simulation study. The forces acting on a vehicle moving along an inclined plane are shown in Fig. 2.7 [6]. The various forces affecting the lateral movement of the vehicle include

- Aerodynamic drag force
- Rolling resistance force
- Weight of the vehicle
- Longitudinal traction force

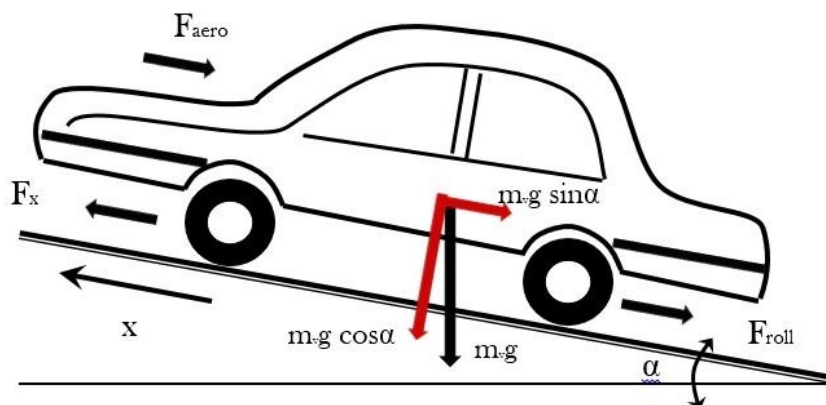


Fig. 2.7. Lateral force components on the vehicle

The algebraic difference between the traction force and the resistive force due to the vehicle load, determines the net force affecting the acceleration or the deceleration of the vehicle. This can be mathematically expressed as

$$F_{acclr} = F_x - F_{aero} - F_{roll} - F_{gravity} \quad (2.1)$$

The longitudinal traction force is based on friction that is proportional to the slip between the tire and the road surface which can be given as

$$F_x = \mu_{s0} s_x m_v g \cos \alpha \quad (2.2)$$

$$s_x = \frac{r_w \omega_w - V_x}{r_w \omega_w}, \text{ is the slip between road and tire surface.} \quad (2.3)$$

The aerodynamic drag force acting upon the vehicle due to the speed of wind is calculated as

$$F_{aero} = \frac{\rho C_d A_f}{2} (V_x + V_{wind})^2 \quad (2.4)$$

With the rotation of the tire, a part of the tire is continually depressed on the bottom and then released back to its original shape as the part of the tire leaves the contact area. This process of depression and releasing are due to damping action. Hence energy is consumed in the process which is reflected as the rolling resistance and opposes the motion of the vehicle. The rolling resistance is typically proportional to the normal gravitational force due to the weight of the vehicle.

$$F_{roll} = f_r m_v g \cos \alpha \quad (2.5)$$

Thus the expression for vehicle dynamic can be written as

$$\frac{dV_x}{dt} = \frac{1}{m_v} \left(\mu_{s0} \frac{r_w \omega_w - V_x}{r_w \omega_w} m_v g \cos \alpha - \frac{\rho C_d A_f}{2} (V_x + V_{wind})^2 - f_r m_v g \cos \alpha - m_v g \sin \alpha \right) \quad (2.6)$$

Therefore the difference between the tractive force and the sum of road loads (gravitational force, rolling resistance and aerodynamic resistance) is used for the purpose of accelerating the vehicle. Here the vehicle is assumed to travel over a horizontal road with the head wind speed being neglected. Hence with $\alpha = 0$ and $V_{wind} = 0$, the simplified expression for Eqn. 2.6 can be given as

$$\frac{dV_x}{dt} = \frac{1}{m_v} \left(\mu_{s0} \frac{r_w \omega_w - V_x}{r_w \omega_w} m_v g - \frac{\rho C_d A_f}{2} V_x^2 - f_r m_v g \right) \quad (2.7)$$

Taking a longitudinal drive line model for the EV as shown in Fig. 2.8 we have

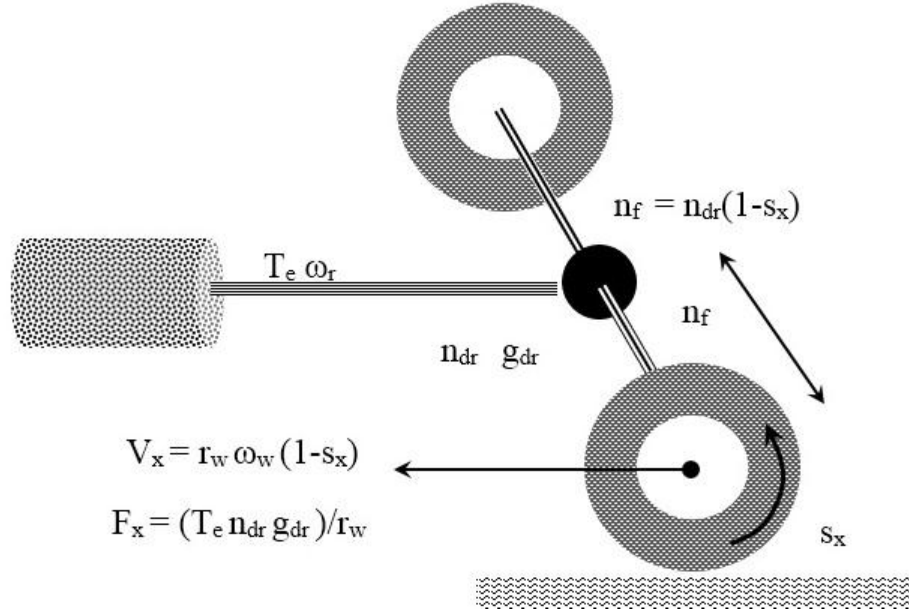


Fig. 2.8. Drive line model of vehicle [6]

$$V_x = r_w \omega_w (1 - s_x) \quad (2.8)$$

$$V_x = r_w \left(\frac{\omega_r}{g_{dr}} \right) (1 - s_x) \quad (2.9)$$

The torque at the motor shaft (T_e) and the torque on the wheel axle (T_w) can be related as

$$T_e \eta_{dr} = \frac{T_w}{g_{dr}} \quad (2.10)$$

The vehicle traction power can be given as

$$P_x = T_w \frac{V_x}{r_w} = T_w \left(\frac{\omega_r}{g_{dr}} \right) (1 - s_x) \quad (2.11)$$

$$P_x = T_e \omega_r \eta_{dr} (1 - s_x) \quad (2.12)$$

The motor shaft power is given as

$$P_e = T_e \omega_r \quad (2.13)$$

The total efficiency between the motor shaft and the vehicle traction system is given as

$$\eta_f = \frac{P_x}{P_e} = \eta_{dr} (1 - s_x) \quad (2.14)$$

The characteristic curve for a traction system, as shown in Fig. 2.2 is composed of two segments of 1) Constant torque region and 2) Constant power region, which are separated by the base speed. With the base speed as the pivot, the maximum tractive effort of EV is set as

$$F_x = \begin{cases} \frac{T_e g_{dr} \eta_{dr}}{r_w}, \omega_r \leq \omega_b \\ \frac{P_e \eta_f}{V_x}, \omega_r > \omega_b \end{cases} \quad (2.15)$$

The governing equation for maximum acceleration in Constant torque region is given as

$$\frac{dV_x}{dt} = \frac{1}{m_v} \left(\frac{T_e g_{dr} \eta_{dr}}{r_w} - f_r m_v g - \frac{\rho C_d A_f}{2} V_x^2 \right) \quad (2.16)$$

while in the constant power region, it is given as

$$\frac{dV_x}{dt} = \frac{1}{m_v} \left(\frac{P_e \eta_f}{V_x} - f_r m_v g - \frac{\rho C_d A_f}{2} V_x^2 \right) \quad (2.17)$$

where, T_e is the electromagnetic torque developed by the motor shaft to drive the vehicle and P_e is the equivalent power developed at motor shaft. The load torque (T_L) acting upon the machine is proportional to load force (F_L) given by Eqn. 2.18. Thus the load torque is proportional to the net resistive force due to aerodynamic drag and rolling resistance, when the vehicle is assumed to be moving on a flat surface.

$$F_L = \left(f_r m_v g + \frac{\rho C_d A_f}{2} V_x^2 \right) \quad (2.18)$$

With respect to Eqn. 2.18, the aerodynamic force (Eqn. 2.4) can be considered very small in comparison to rolling resistance force (Eqn. 2.5). Under this assumption, it can be concluded that the load acting upon the traction motor is proportional to the mass of the vehicle. Hence the vehicle load can be considered to be constant for simplification of analysis.

2.3 INDUCTION MACHINE MODEL

2.3.1 Steady State Operation of Induction Machine

For a 3- Φ IM, the power slip characteristic and torque slip characteristic [9, 10] governed by the Eqn. 2.19 and Eqn. 2.20 are represented in Fig. 2.9 and Fig. 2.10 respectively.

$$P = \frac{3V_1^2}{\left(r_1 + \frac{r_2}{s}\right)^2 + (x_1 + x_2)^2} \cdot r_2 \left(\frac{1-s}{s}\right) \quad (2.19)$$

$$T_e = \frac{3}{\omega_s} \cdot \frac{V_1^2}{\left(r_1 + \frac{r_2}{s}\right)^2 + (x_1 + x_2)^2} \cdot \frac{r_2}{s} Nm \quad (2.20)$$

From the characteristic curve it can be observed that induction machines have three modes of operation, namely (1) Motoring Mode ($0 < s \leq 1$), (2) Generating Mode ($s < 0$) & (3) Braking Mode ($s > 1$).

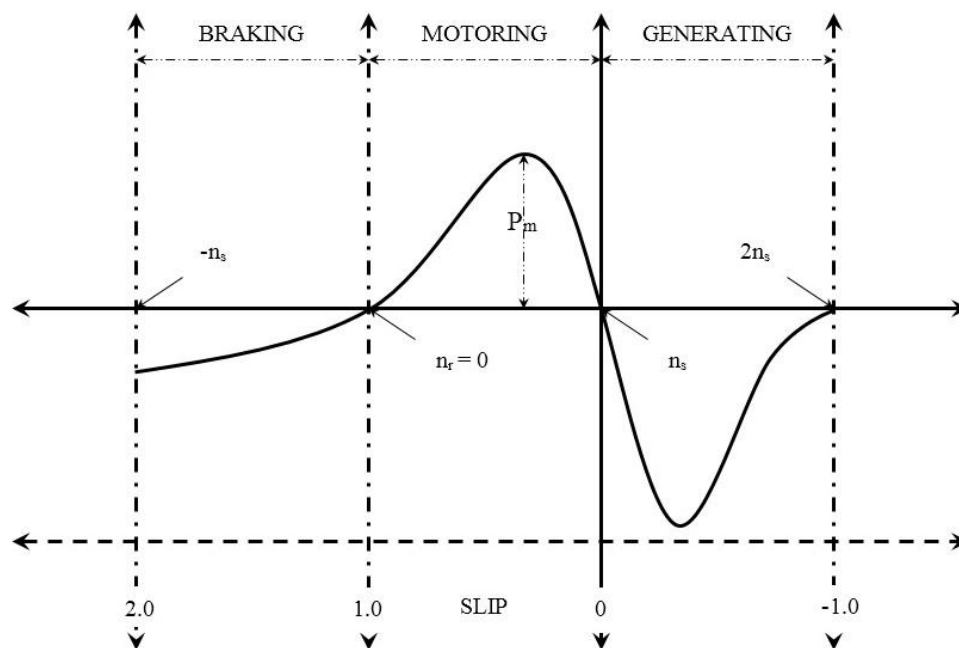


Fig. 2.9. Power slip characteristics of induction machine

Generally, in the braking region the power is shown to be negative and the torque is positive as shown in Fig. 2.9 and Fig. 2.10. However, in the present research work the plug

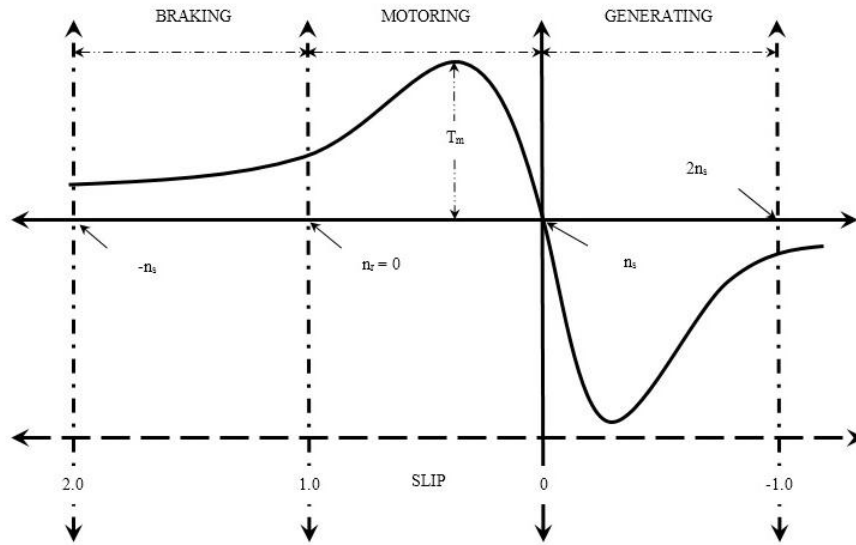


Fig. 2.10. Torque slip characteristics of induction machine

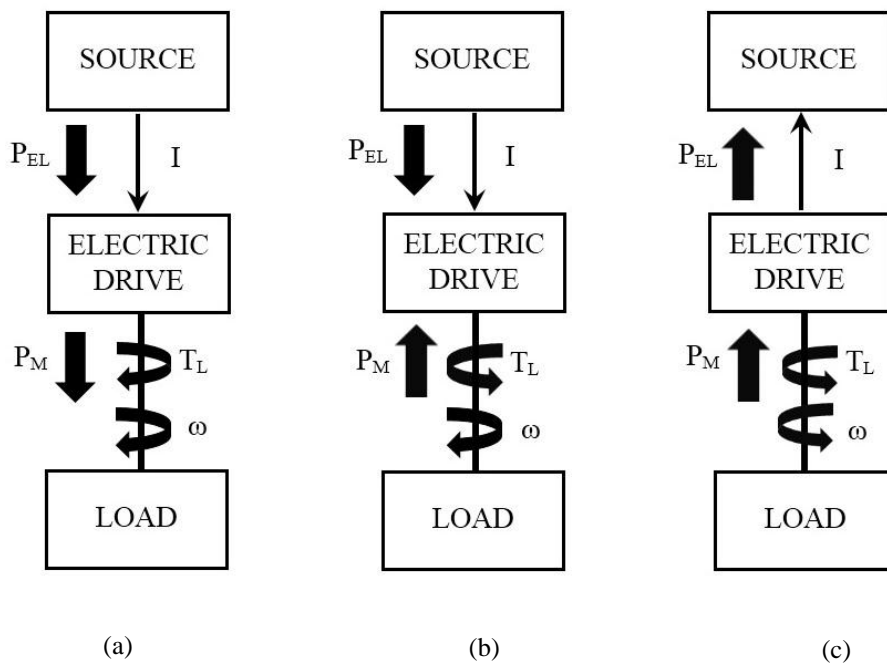


Fig. 2.11. Modes of operation in induction machine

(a) Motoring (b) Braking (c) Generating

braking operation is manifested by reversing the direction of the Rotating Magnetic Field (RMF) directly. Hence the nature of power and torque in the braking region reverses from the actual practice. Therefore, the machine operates in the braking region with negative torque. However, there is no regeneration of power in this region and hence this kinetic energy goes waste. The IM can be made to operate through the regenerative braking mode by driving the

machine with negative slip. This is achieved by maintaining the frequency of RMF always below the frequency corresponding to rotor speed by the use of variable frequency drives. Thereby a negative torque as well as a negative power is produced as shown in Fig. 2.11 (c). The negative torque is envisaged as the braking torque and the negative power is regenerated [30] into the battery.

2.3.2 Dynamic Modeling of Induction Machine

In the conventional system of the 3Φ drive, a converter circuit is used between the battery and the machine. The switching phenomenon of the inverter generates harmonics which are filtered using LC filters. The three phase system of IM is complicated for mathematical analysis and modeling, as rotor windings move with respect to stator windings. The analysis is also complex due to the presence of time varying inductances [11]. In this research work, the braking process is analyzed using the dynamic model of the IM. This facilitates a simpler analysis of the dynamic performance of the machine both in steady-state and transient conditions. The IM model in synchronously rotating reference frame additionally gives a modular approach.

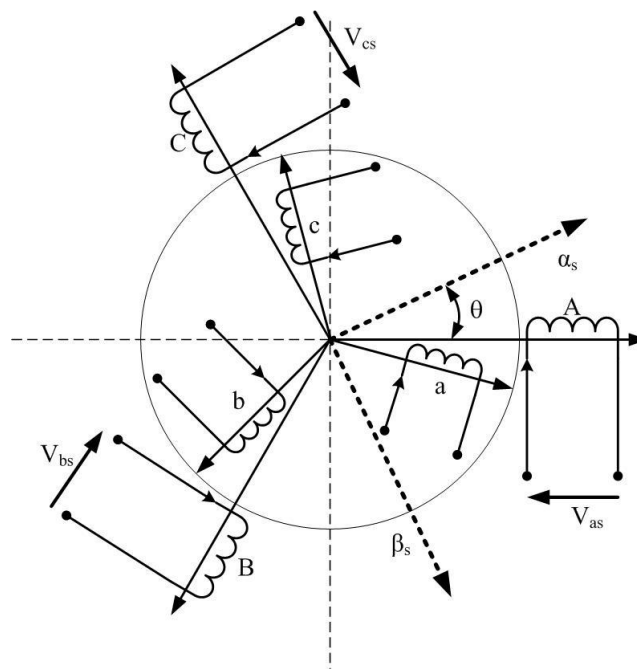


Fig. 2.12. Three phase stationary reference frame

Considering a symmetrical 3Φ IM as shown in the Fig. 2.12, the stationary stator axes as-bs-cs are displaced by a phase angle of $\frac{2\pi}{3}$. Initially, 3Φ stationary reference frame variables (a-b-c) are transformed to 2Φ stationary reference frame variables (α - β -0) and then to synchronously rotating reference frame variables (d-q-0) [11-13]. Inverse transformations are used to obtain the three phase variables from the synchronously rotating frame variables.

The linear transformation between the 3Φ stationary frame and the 2Φ stationary frame is given by

$$\mathbf{f}_{\alpha\beta 0} = [\mathbf{K}_s] \mathbf{f}_{abc} \quad (2.21)$$

$$\mathbf{K}_s = \begin{bmatrix} \cos \theta & \cos\left(\theta - \frac{2\pi}{3}\right) & \cos\left(\theta - \frac{4\pi}{3}\right) \\ \sin \theta & \sin\left(\theta - \frac{2\pi}{3}\right) & \sin\left(\theta - \frac{4\pi}{3}\right) \\ \frac{1}{2} & \frac{1}{2} & \frac{1}{2} \end{bmatrix} \quad (2.22)$$

And the inverse transformation matrix is given as

$$\mathbf{K}_s^{-1} = \begin{bmatrix} \cos \theta & \sin \theta & 1 \\ \cos\left(\theta - \frac{2\pi}{3}\right) & \sin\left(\theta - \frac{2\pi}{3}\right) & 1 \\ \cos\left(\theta - \frac{4\pi}{3}\right) & \sin\left(\theta - \frac{4\pi}{3}\right) & 1 \end{bmatrix} \quad (2.23)$$

The transformation of the 2Φ stationary reference frame to the synchronously rotating reference frame is given by the matrix

$$\begin{bmatrix} i_d \\ i_q \end{bmatrix} = \begin{bmatrix} \cos \theta & \sin \theta \\ -\sin \theta & \cos \theta \end{bmatrix} \begin{bmatrix} i_\alpha \\ i_\beta \end{bmatrix} \quad (2.24)$$

The electrical transient model of induction machine in the dq system in terms of voltages and currents can be given in the form of

$$\begin{bmatrix} v_{qs} \\ v_{ds} \\ v_{qr} \\ v_{dr} \end{bmatrix} = \begin{bmatrix} R_s + pL_s & \omega_e L_s & pL_m & \omega_e L_m \\ -\omega_e L_s & R_s + pL_s & -\omega_e L_m & pL_m \\ pL_m & (\omega_e - \omega_r) L_m & R_r + pL_r & (\omega_e - \omega_r) L_r \\ -(\omega_e - \omega_r) L_m & pL_m & -(\omega_e - \omega_r) L_r & R_r + pL_r \end{bmatrix} \begin{bmatrix} i_{qs} \\ i_{ds} \\ i_{qr} \\ i_{dr} \end{bmatrix} \quad (2.25)$$

$$v_{qs} = R_s i_{qs} + \frac{d}{dt} \psi_{qs} + \omega_e \psi_{ds} \quad (2.26)$$

$$v_{ds} = R_s i_{ds} + \frac{d}{dt} \psi_{ds} - \omega_e \psi_{qs} \quad (2.27)$$

$$v_{qr} = R_r i_{qr} + \frac{d}{dt} \psi_{qr} + (\omega_e - \omega_r) \psi_{dr} \quad (2.28)$$

$$v_{dr} = R_r i_{dr} + \frac{d}{dt} \psi_{dr} - (\omega_e - \omega_r) \psi_{qr} \quad (2.29)$$

Here p represents the time derivative of the expression. Considering the constant inertia load, the electrical dynamics of the machine are given by fourth order linear system.

The speed ω_r is dependent on torque and is expressed as

$$T_e = T_L + J \frac{d\omega_m}{dt} = T_L + \frac{2}{P} J \frac{d\omega_r}{dt} \quad (2.30)$$

The vector representation of torque is given as

$$T_e = \left(\frac{3}{2}\right) \left(\frac{P}{2}\right) [\overline{\Psi}_m \times \overline{I}_r] \quad (2.31)$$

which can also be represented as

$$T_e = \left(\frac{3}{2}\right) \left(\frac{P}{2}\right) L_m (i_{qs} i_{dr} - i_{ds} i_{qr}) \quad (2.32)$$

The equivalent circuit of the dq model of the induction machine can be represented through q-axis and d-axis as shown in Fig. 2.14.

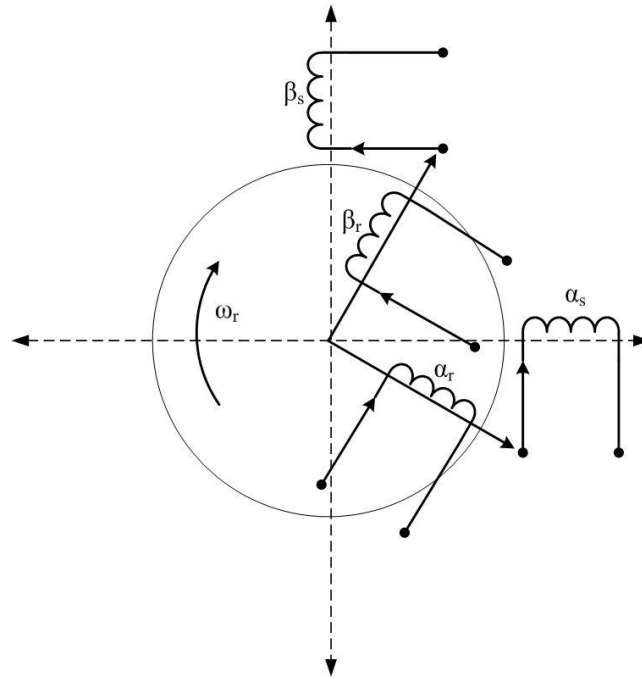


Fig. 2.13. Two phase stationary reference frame

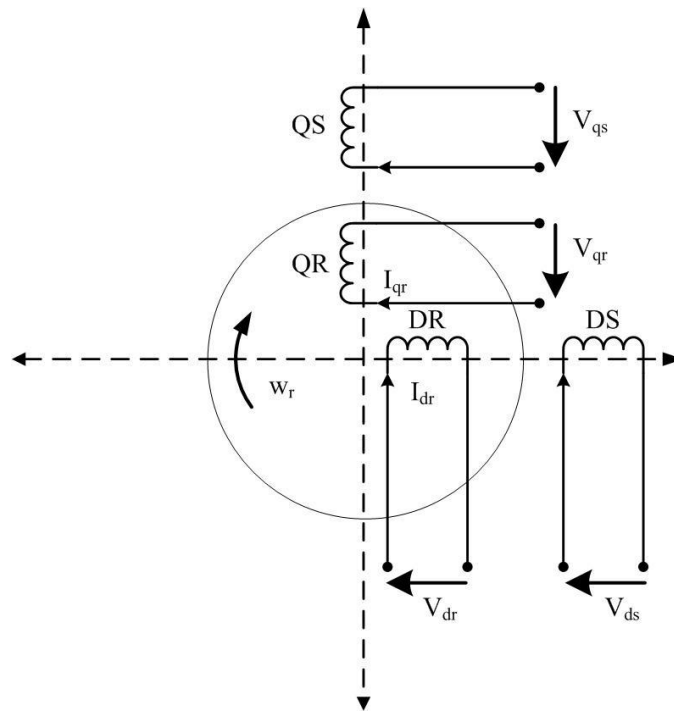


Fig. 2.14. Synchronously rotating reference frame

The expression for flux linkages are given as

$$F_{qs} = \omega_b \psi_{qs} = X_{ls} i_{qs} + X_m (i_{qs} + i_{qr}) \quad (2.33)$$

$$F_{qr} = \omega_b \psi_{qr} = X_{lr} i_{qr} + X_m (i_{qs} + i_{qr}) \quad (2.34)$$

$$F_{ds} = \omega_b \psi_{ds} = X_{ls} i_{ds} + X_m (i_{ds} + i_{dr}) \quad (2.35)$$

$$F_{dr} = \omega_b \psi_{dr} = X_{lr} i_{dr} + X_m (i_{ds} + i_{dr}) \quad (2.36)$$

$$F_{qm} = X_{ml} \left[\frac{F_{qs}}{X_{ls}} + \frac{F_{qr}}{X_{lr}} \right] \quad (2.37)$$

$$F_{dm} = X_{ml} \left[\frac{F_{ds}}{X_{ls}} + \frac{F_{dr}}{X_{lr}} \right] \quad (2.38)$$

where

$$\frac{1}{X_{ml}} = \frac{1}{X_m} + \frac{1}{X_{ls}} + \frac{1}{X_{lr}} \quad (2.39)$$

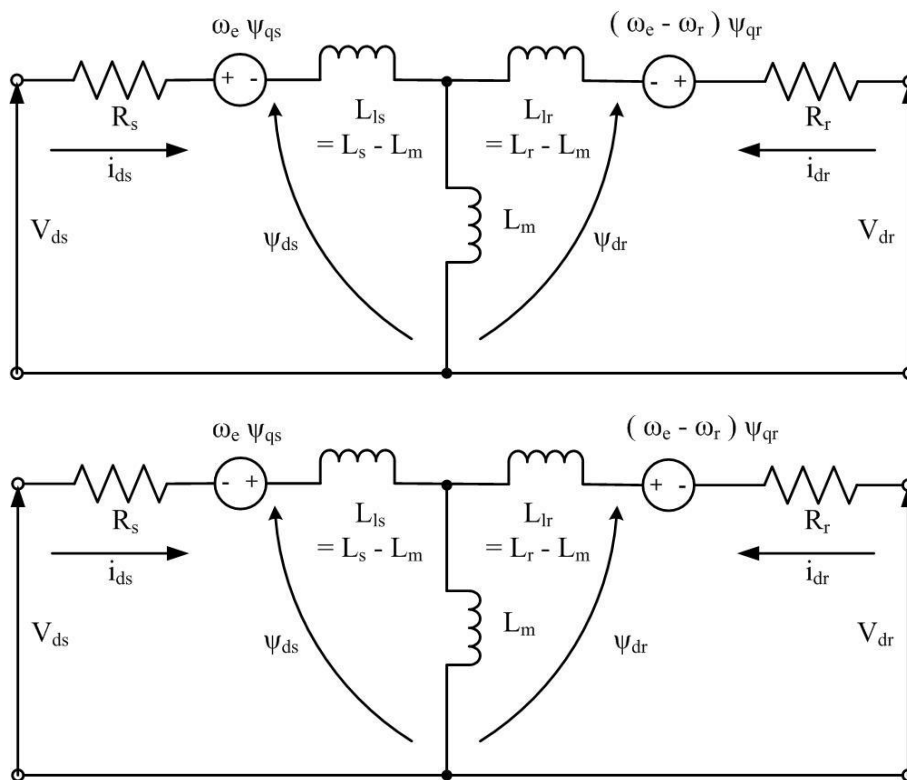


Fig. 2.15. Dynamic or d-q equivalent circuit of induction machine

The machine currents being produced in the two phase system in terms of flux linkage are expressed as

$$i_{qs} = \frac{1}{X_{ls}} (F_{qs} - F_{qm}) \quad (2.40)$$

$$i_{ds} = \frac{1}{X_{ls}} (F_{ds} - F_{qm}) \quad (2.41)$$

$$i_{qr} = \frac{1}{X_{lr}} (F_{qr} - F_{qm}) \quad (2.42)$$

$$i_{dr} = \frac{1}{X_{lr}} (F_{dr} - F_{qm}) \quad (2.43)$$

The state space model of the induction machine under dynamic conditions is given by

$$\frac{dx}{dt} = Ax + B \quad (2.44)$$

The state variables can be represented in the form of state vector given as

$$x = [F_{qs} \ F_{ds} \ F_{qr} \ F_{dr} \ \omega_r]^T \quad (2.45)$$

Hence the governing equations of a squirrel cage IM can be represented in the state space form which are given as [12]

$$\frac{dF_{qs}}{dt} = \omega_b \left[v_{qs} - \frac{\omega_e}{\omega_b} F_{ds} - \frac{R_s}{X_{ls}} (F_{qs} - F_{qm}) \right] \quad (2.46)$$

$$\frac{dF_{ds}}{dt} = \omega_b \left[v_{ds} + \frac{\omega_e}{\omega_b} F_{qs} - \frac{R_s}{X_{ls}} (F_{ds} - F_{dm}) \right] \quad (2.47)$$

$$\frac{dF_{qr}}{dt} = -\omega_b \left[v_{qr} + \frac{(\omega_e - \omega_r)}{\omega_b} F_{dr} + \frac{R_r}{X_{lr}} (F_{qr} - F_{qm}) \right] \quad (2.48)$$

$$\frac{dF_{dr}}{dt} = -\omega_b \left[v_{dr} - \frac{(\omega_e - \omega_r)}{\omega_b} F_{qr} + \frac{R_r}{X_{lr}} (F_{dr} - F_{dm}) \right] \quad (2.49)$$

$$\frac{d\omega_r}{dt} = \left(\frac{P}{2J} \right) (T_e - T_L) \quad (2.50)$$

These equations are well accepted for mathematical modeling as they are helpful in analysing the transient performance of IM. These equations also establish an appropriate relationship between the electrical parameters (voltage and current) and the mechanical parameters (speed and torque). For a singly fed squirrel cage induction machine we have, $v_{qr} = v_{dr} = 0$. An IM of the rating of the order of 40 - 50 hp is implemented as the traction drive [38]. In the present research work two IMs of different ratings are used to analyse the improved braking performance of a hybrid electric braking system. The main traction motor of rating 3- Φ , 460-V, 50-hp, 60-Hz, 4-pole (Table II, Appendix 2) is used for regenerative braking and an auxiliary motor of rating 3- Φ , 220-V, 3-hp, 60-Hz, 4-pole (Table III, Appendix 2) is used for plug braking. The parameter details of both the motors are taken from [12]. The mathematical model given by Eqn. 2.46 to Eqn. 2.50 is initially validated for 3 hp motor by comparing its dynamic behaviour during no load conditions. The friction and windage losses are also neglected considering an ideal operation. A voltage of 220 V is applied as input to the q- axis model while input to the d-axis model is kept at 0 V (short-circuited). The variation of the machine speed and the torque speed characteristics during starting are illustrated in Fig. 2.16 and Fig. 2.17 respectively.

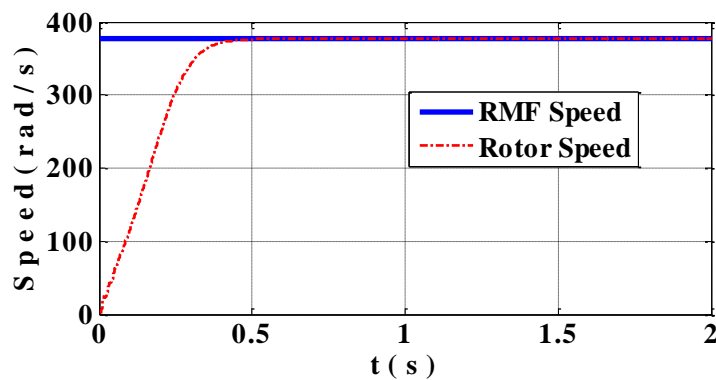


Fig. 2.16. Comparison of rotor speed with RMF speed

The rotating magnetic field (RMF) has a rated value of 377 rad/s (electrical speed). The rotor is started from rest i.e. 0 rad/s and gradually attains the rated speed of RMF in $t = 0.5$ s. The speed of the rotor follows the RMF speed. The variation of electromagnetic torque output of the machine with speed is shown in Fig. 2.17. The torque output of the machine becomes 0 N-m at the rated speed, i.e. 377 rad/s. This analysis of starting period is demonstrated entirely in the motoring mode. The study is in aptness with the results shown in [12], [13].

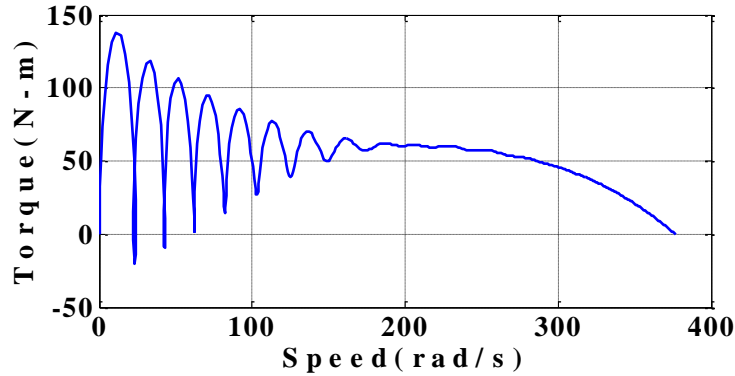


Fig. 2.17. Variation of torque with speed

2.4 BATTERY MODEL

For the purpose of EVs and HEVs, batteries are the primary means of energy storage. In the use of HEVs, rechargeable batteries are used which deliver energy to the machine system (discharging) while cruising, accept energy from the system (charging) during regenerative braking and also store energy when not in use (storage). For the application in automobile industries, batteries should be efficient in terms of specific power, specific energy, efficiency, safety, cost, maintenance requirement and environmental adaptability.

The two primary modeling strategies for the battery are the circuit oriented modeling and the mathematical modeling [17]. Circuit oriented battery models use a combination of voltage and current sources, resistors and capacitors to model the battery performance. The various basic forms include the

1. Thevenin Based Model
2. Impedance Based Model
3. Runtime Based Model

However, such models are complicated enough to determine battery parameters and the state of charge of the battery in account for variations between the charge and the discharge state which requires two opposing diodes. This makes the system even more complex. The mathematical modeling is based on Shepherd Equation and Peukerts Model. The voltage-current model describing the change of the terminal voltage with respect to current is the most vital sub model. This model usually starts from the basic Shepherd Equation and then the relation is improved to fit to the charge and discharge curve (Fig. 2.18). Here mathematical model of the lithium ion battery which is most widely used for applications in EVs and HEVs

has been used. The battery voltage, the battery current and the state of charge (SOC) of the battery are chosen as state variables to depict the performance of the battery both during the charging and the discharging phenomenon.

The Shepherd model describes the electrochemical behaviour of the battery in terms of the terminal voltage, open circuit voltage, internal resistance, discharge current and state of charge [17]. This model is well defined for both the charge and the discharge characteristics. The mathematical model based on Shepherd Model available in MATLAB/SimPowerSystems for Li-Ion model has been used here.

$$\text{Charge: } V_{batt} = E_o - R \times i - K \times \left(\frac{Q}{it - 0.1 \times Q} \right) \times i^* - K \times \left(\frac{Q}{Q - it} \right) \times it + A \exp(-B \times it) \quad (2.51)$$

$$\text{Discharge: } V_{batt} = E_o - R \times i - K \times \left(\frac{Q}{Q - it} \right) \times (it + i^*) + A \exp(-B \times it) \quad (2.52)$$

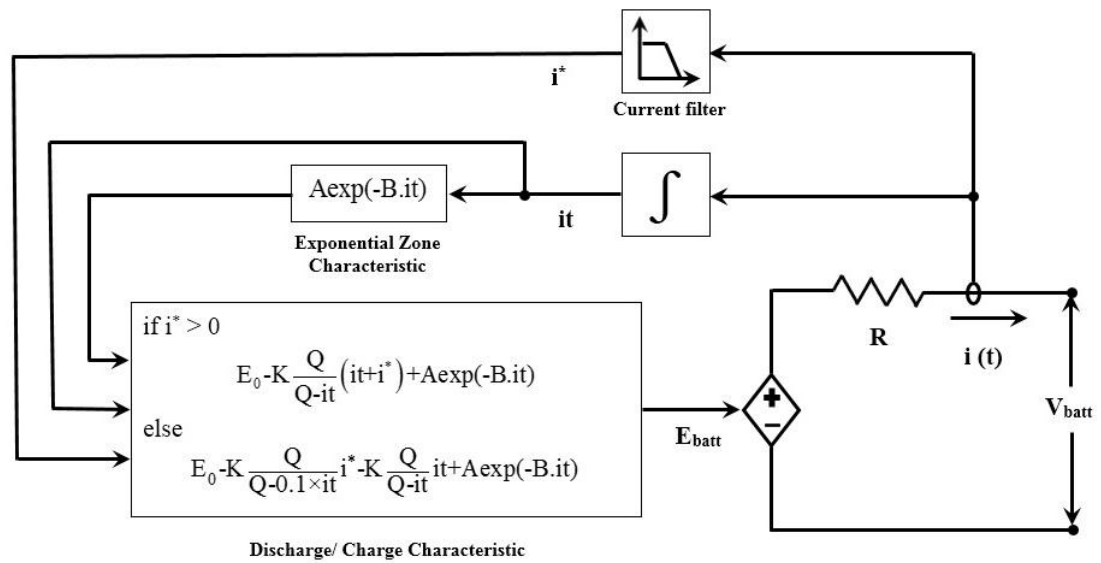


Fig. 2.18. Nonlinear battery model

$$K \times \left(\frac{Q}{Q - it} \right) \times it = \text{Polarization Voltage}$$

$$K \times \left(\frac{Q}{Q - it} \right) = \text{Polarization resistance}$$

The state of charge (SOC) of the battery can be given by

$$SOC = 1 - \frac{it}{Q}; \quad (2.53)$$

The equivalent block diagram for the nonlinear Li-Ion battery model (Fig. 2.18) has been shown in Fig. 2.19.

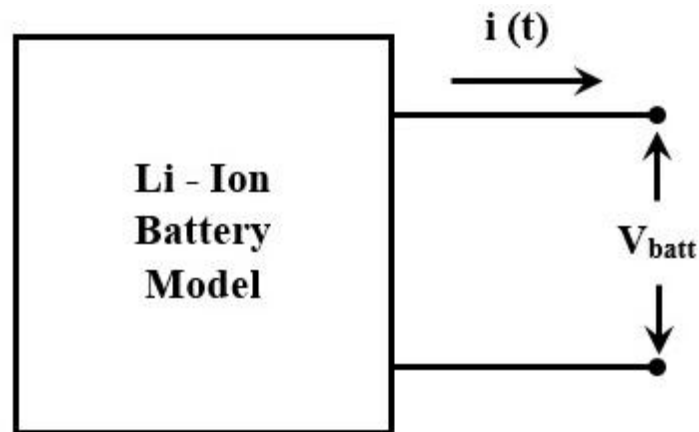


Fig. 2.19. Equivalent block diagram of Li-Ion battery model

The following assumptions are made in the modeling of the battery

- During both charging and discharging the internal resistance remains constant and independent of the amplitude of the current.
- The parameters are extracted from the discharge characteristics and are assumed to remain the same for charging.
- The battery capacity remains independent of the amplitude of the current. (No Peukert Effect)
- The temperature has no effect on the behavior of the model.
- The self-discharge of the battery is not represented.
- There is no memory effect on the model.

The following are the limitations in the design of the battery model

- The minimum no load battery voltage is 0 V and the maximum voltage is $2 \times E_0$ V.
- The minimum capacity of the battery is 0 Ah and the maximum capacity is Q.
- The maximum SOC cannot be greater than 100 % if the battery is over-charged.

The above assumptions are theoretically accepted but the minimum limitation SOC in the industrial sector is varied between 20 – 40 %. The lithium is the lightest of metals and also

presents proper electrochemical characteristics. Because of its listed advantages in [1], a Li-Ion battery model has been used as the energy source for this thesis work. Taking a battery with nominal voltage = 3.3 V, rated capacity = 2.3 Ah and battery response time of 30 s as given in [20], the discharge curve is used to extract the parameters E_o , R , K , A , and B .

- E_o = 3.366 V
- R = 0.01 Ω
- K = 0.0076 V/(Ah)
- A = 0.26422 V
- B = 26.5487 (Ah)⁻¹

The 50 hp main motor requires a supply voltage of 460 V and the 3 hp auxiliary motor requires a supply of 220 V. Taking the Li-Ion battery of 3.3 V as discussed earlier in this section, the required voltages of 220 V and 460 V can be obtained by building up battery packs by combining a number of 3.3 V Li-Ion batteries as required. Thus the parameters of the discharge characteristics of these battery packs can be mathematically obtained as discussed in Appendix 3.

2.5 SUMMARY

In this chapter the vehicle performance is studied using the equations of vehicle dynamics. The various configurations and features of the EVs/HEVs are examined from the literature. Based on this preliminary knowledge the traction characteristic of the vehicle is outlined. From this initial analysis of lateral dynamics, the vehicle load affecting the traction motor has been introduced. Thereafter the electric propulsion system and its energy storage devices are discussed. With a view to the basic structure, performance, control and operational characteristics described in aptness with the traction system, the induction machine is found to be the best performer for the vehicle dynamics. A study based on the different types of the energy storage technologies is also carried out. A proper selection of the battery parameters and its proper modeling is quite essential for its use as the power source for the electrical machine engulfed in the traction system of the vehicle. The dynamic modeling enabled a simpler method of interfacing the battery with the machine for study of transients during braking of vehicle.

CHAPTER 3
BRAKING ANALYSIS OF AN ELECTRIC VEHICLE
WITH INDUCTION MOTOR DRIVE

INTRODUCTION

PLUG BRAKING ANALYSIS OF IM

REGENERATIVE BRAKING ANALYSIS OF IM

SUMMARY

3.1 INTRODUCTION

As already discussed in the previous chapters, braking may be employed while withdrawing the kinetic energy from the wheels or while dissipating the kinetic energy. During plug braking entire energy is dissipated in the machine and during regenerative braking energy is fed back to the source. However, the magnitude of retardation varies in each case. In this chapter, a simulation study is performed using MATLAB by considering above two types of braking separately. Field oriented control (FOC) is used in the case of regenerative braking and voltage oriented control (VOC) in the case of plug braking [39 - 41]. These results are useful in combining both the types of braking to obtain hybrid electric braking to be discussed in the next chapter.

3.2 PLUG BRAKING ANALYSIS OF IM

3.2.1. Voltage Oriented Control

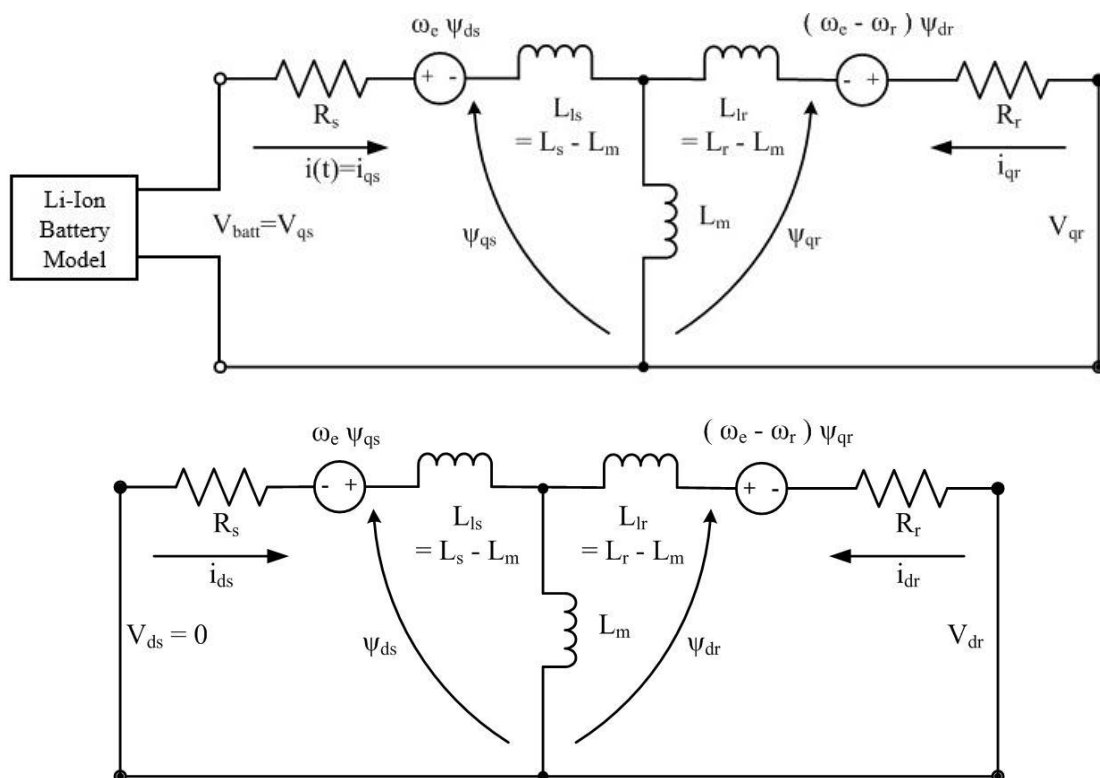


Fig. 3.1. Dynamic model of induction machine using voltage oriented control

In the present research work, the dynamic dq model of the IM has been used for braking analysis. Voltage oriented control has been adopted so as to simplify the analysis as shown in Fig. 3.1. The voltage along the d-axis input terminals are taken to be zero with proper

orientation so as to apply FOC. A battery connected to IM is equivalent to connecting battery model shown in Fig. 2.19 at the input terminal of q-axis equivalent circuit of dynamic model of IM. This gives an equation $v_{qs} = V_{\text{batt}}$, and $i(t) = i_{qs}$, that establishes a mathematical relation between the battery model and IM model. This model is used to analyze transients during plugging in IM and it is used for the auxiliary motor. Generally the plug braking operation for a 3 Φ IM is obtained by reversing the sequence of any two phases of the three phase supply terminals, which reverses the direction of the rotating magnetic field. In analysis with the dynamic model of the induction machine, plug braking is obtained by simply replacing ω_e by $-\omega_e$ which is equivalent to reversing the direction of the rotating magnetic field (RMF). The speed of the RMF is taken as the braking command.

3.2.2. Results and Discussion

The plug braking analysis is carried on a 3- Φ , 220-V, 3-hp, 60-Hz, 4-pole IM (auxiliary motor). The traction motor is driven by a constant vehicle load which is equivalent to the rated load of the machine. Simulation is performed using MATLAB with ‘ode45’ differential equations solver. The variation of the rotor speed is shown in Fig. 3.2. Initially the machine starting as motor with the given constant load, rotates with 2 percent slip. The time ‘t’ in seconds shown on the x-axis has been considered after the machine reaches the steady state speed. The RMF speed is changed from 377 rad/s to -377 rad /s at $t = 0.1$ s, to be used as a braking command. With the reversal of RMF speed, the rotor speed gradually falls back and finally attains zero speed at $t = 0.34$ s. However, at this instant, the stator supply is required to be disconnected or else the machine picks up negative speed. A mechanical device is assumed to stop the vehicle from going in reverse direction.

Fig. 3.3 shows the variation of torque in the plugging operation. With the application of brakes the machine produces a braking torque. The initial peak of the pulsating torque is around -500 N-m. Fig. 3.4 and Fig. 3.5 show the variation of battery voltage and current respectively at the instant of plug braking. The battery voltage during plug braking decreases from its normal rated value. Moreover, during the braking process, the average value of current is positive and hence the power developed during this braking is wasted in the machine itself. This indicates the wastage of energy during braking process without any regeneration.

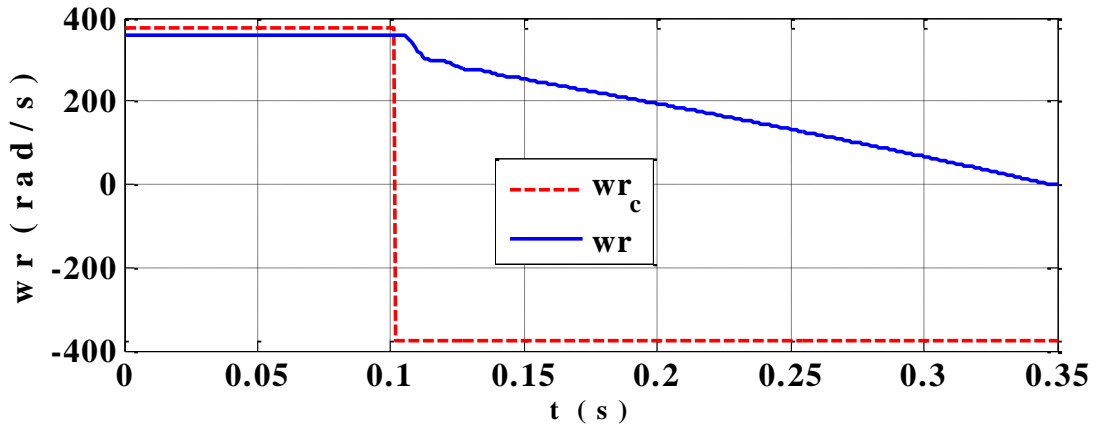


Fig. 3.2. Variation of speed during plug braking

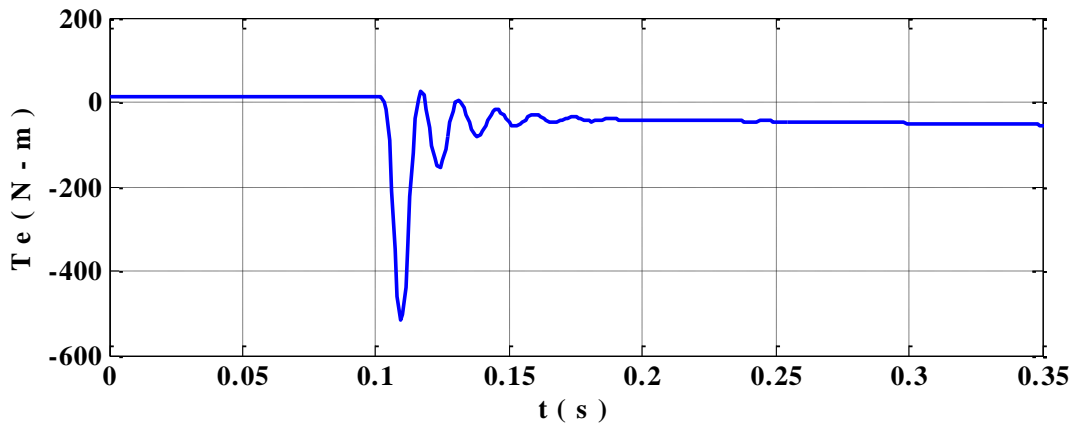


Fig. 3.3. Variation of torque during plug braking

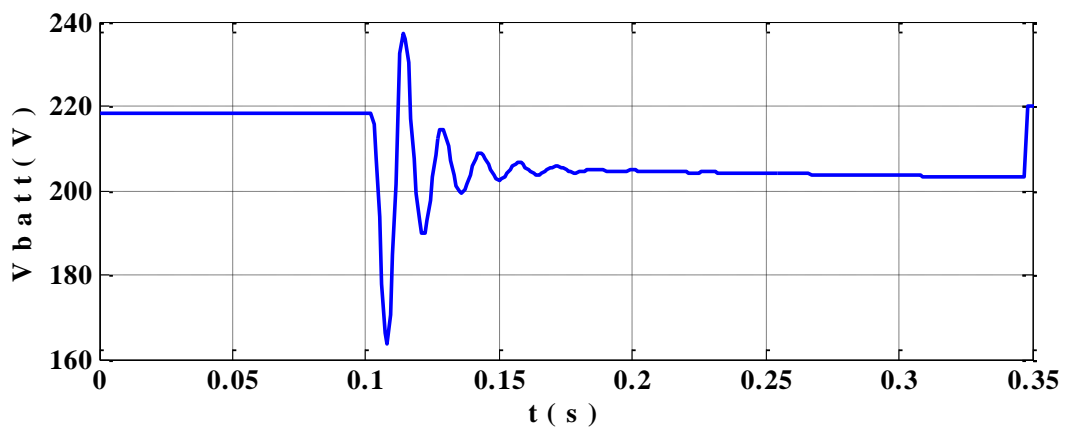


Fig. 3.4. Variation of battery voltage during plug braking

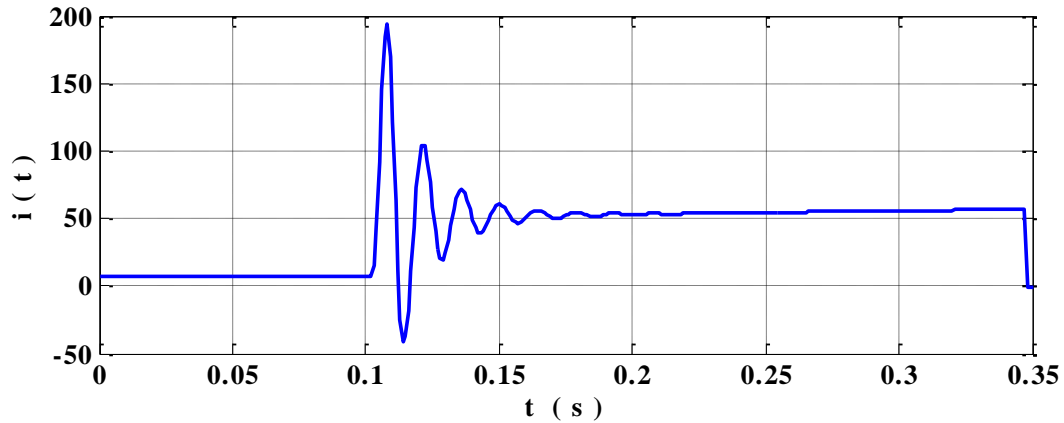


Fig. 3.5. Variation of battery current during plug braking

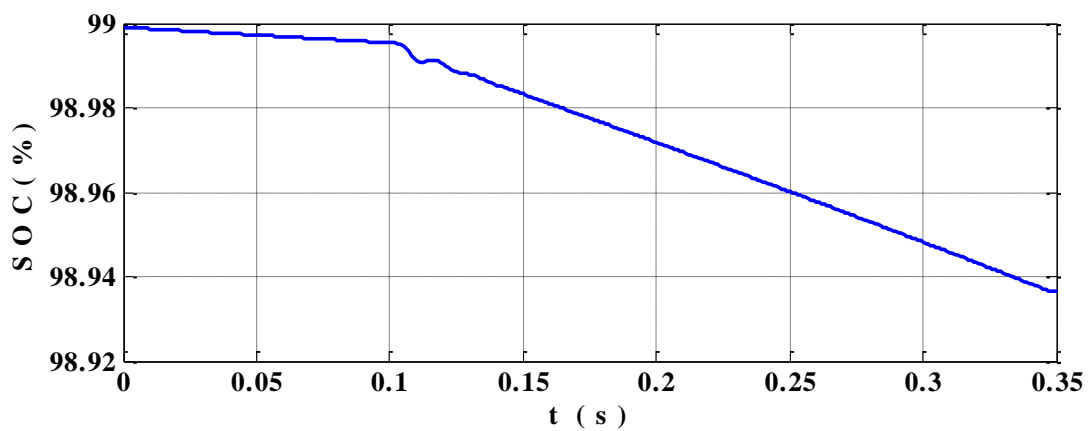


Fig. 3.6. Variation of SOC during plug braking

The battery interfaced with the machine shows the variation of the state of charge (SOC) in Fig. 3.6. Before the instant of braking at $t = 0.1$ s, there is the fall of SOC up to 98.99% as the battery is supplying the machine in the motoring mode. Also, after the brakes are applied the SOC falls drastically from 98.99 % to 98.94 %. This shows that the slope of SOC during plug braking is very high in comparison to the SOC during steady state rated operation. This sudden fall in SOC show that battery is loaded heavily during plug braking. Both voltage and current are seen to have high magnitudes with pulsating nature in Fig. 3.4 and Fig. 3.5. Initially the machine is running as motor, so as it is drawing power from the battery, the voltage is shown to be 218 V up to $t = 0.1$ s. Under the effect of plug braking the machine is drawing more power, hence the battery voltage is dropped to 200 V. Beyond $t = 0.34$ s, after the machine has come to rest the battery voltage restores to the rated value of 220 V as the machine is disconnected from the supply as it attains zero speed. The peak magnitude of pulsating transient current tends to be around 200 A which is around 16 times larger than the value of rated current. Such high magnitudes of the pulsating current can be limited by

connecting external resistance in series with the rotor circuit. In simulation study it has been analysed that the oscillations during plug braking are reduced by the use of external resistance. The pulsating nature of torque can be nominally reduced by this method. As the machine is about to attain zero speed, the supply terminals are disconnected so as to prevent any internal losses.

3.3 REGENERATIVE BRAKING ANALYSIS OF IM

Although the plug braking method is an efficient method of instantaneous braking, but there is no restoration of energy in the process. The entire energy is wasted as thermal energy. Hence, as a suitable alternative, regenerative braking has been introduced. Although the effectiveness of braking in terms of fastness has been decreased with regenerative braking in comparison to plugging but the restoration of power and energy during braking into the battery makes it more efficient for vehicle dynamics. Regenerative braking mode can be achieved by driving the machine with negative slip, by the use of variable frequency drives. The process of regeneration also requires to develop the desired braking torque as commanded by the driver. During transient conditions like braking in vehicles, vector control of IM gives proper torque control. Hence field oriented control (FOC) algorithm has been used.

3.3.1 *Field Oriented Control*

The high performance application of induction machine drives for use in EVs and HEVs require greater reliability. Here the drive is required to act as a torque transducer where the electromagnetic torque is instantaneously made equal to the torque command [12]. These requirements are successfully accessed through vector control or field oriented control.

The basic performance of the field oriented control can be described using a current loop in a uniform flux and analyzing it through Lorentz force equation shown in Fig. 3.7. The torque being produced by the current carrying loop in the magnetic field is given as

$$T_e = - 2 B i N L r \sin \theta \quad (3.1)$$

- B : flux density
- i : current in the coil
- L : length of the coil
- r : radius of coil
- N : number of turns

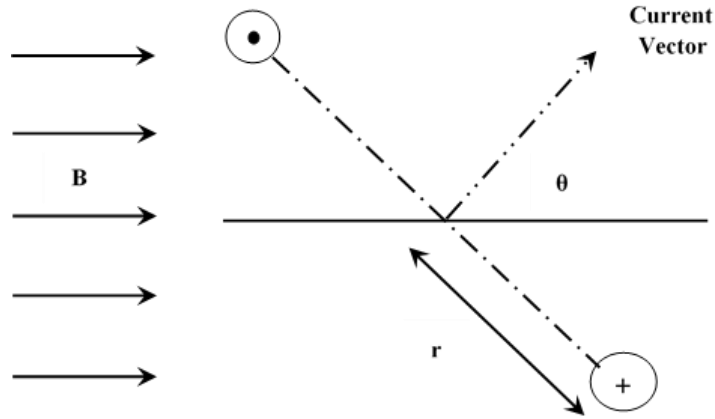


Fig. 3.7. Torque production in a current loop

The torque will be maximized when the current vector is defined orthogonal to the surface of the flux produced. Similarly, in an induction machine the torque is expressed as a vector product of the flux vector and the current vector defined as

$$T_e = -\frac{3P}{2} |\lambda_{qdr}| |i_{qdr}| \sin \theta \quad (3.2)$$

which can be maximized when the flux linkage and the current vectors are perpendicular. The algorithm thus implemented to obtain such a performance of the IM is collectively known as field oriented control. The basic method of FOC is classified as direct method and indirect method depending on the method of determining the flux angle. In field oriented control the entire flux of the machine is aligned along the d- axis and the flux along q- axis is taken to be zero as shown in Fig. 3.8

The method of FOC is governed by two strategies. The first condition is to have

$$\lambda_{qr} = 0 \quad (3.3)$$

and the second strategy is given as

$$i_{dr} = 0 \quad (3.4)$$

When the strategies in Eqn. 3.3 and Eqn. 3.4 hold, then the rotor flux linkage and the rotor current vectors are perpendicular to each other, both during transient and steady state conditions. Under these conditions the torque is maximized. The equivalent dynamic model for IM implementing FOC has been shown in Fig. 3.8.

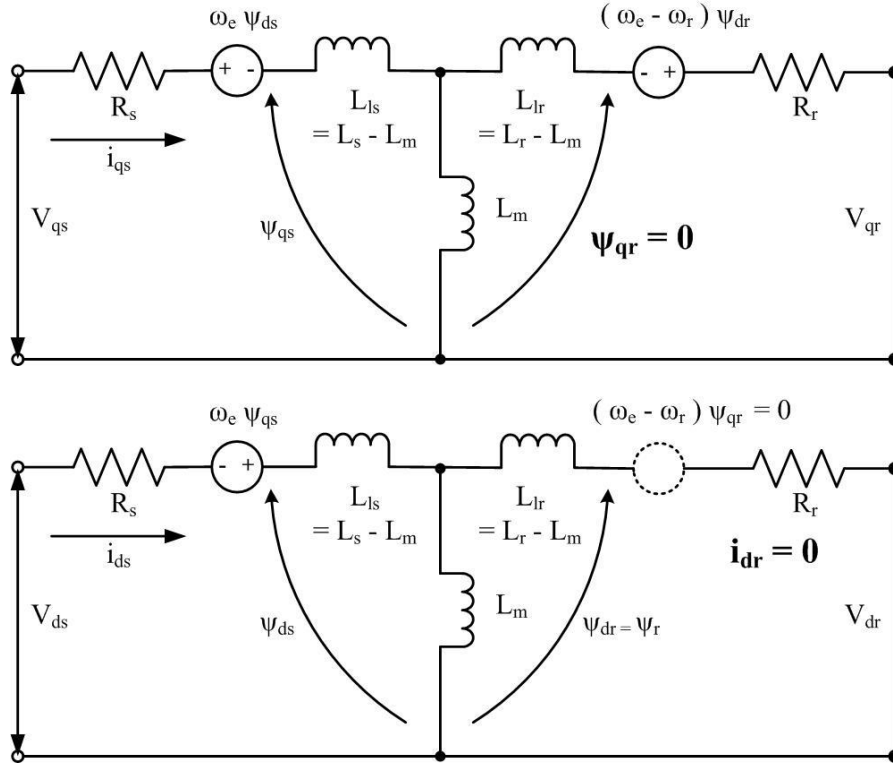


Fig. 3.8. Dynamic or d-q equivalent circuit of induction machine with field oriented control

A block diagram representation of direct FOC in 3 Φ IM is shown in Fig. 3.9. For proper field orientation and controlling the switching of the inverter, the first strategy of $\lambda_{qr} = 0$ is obtained by estimating the rotor flux. The rotor flux is estimated from the measured air gap flux (λ_{qm}^s and λ_{dm}^s) and stator currents i_{qs}^e and i_{ds}^e using the Eqn. 3.5 and Eqn. 3.6.

$$\lambda_{qr}^s = \frac{L_{rr}}{L_m} \lambda_{qm}^s - L_{lr} i_{qs}^s \quad (3.5)$$

$$\lambda_{dr}^s = \frac{L_{rr}}{L_m} \lambda_{dm}^s - L_{lr} i_{ds}^s \quad (3.6)$$

The second strategy of $i_{dr} = 0$ is obtained by forcing the stator current in d-axis i_{ds}^e to remain constant. The stator current in d-axis (i_{ds}^e) and q-axis (i_{qs}^e) are decoupled like the field current and armature current of the DC machine respectively. The d-axis current controls the flux of the IM and the q-axis current controls the electromagnetic torque. Hence by giving a negative torque command and ensuring that the direction of ω_e is not negative, the machine is bound to operate in regenerative braking mode with maximum braking torque. This technique

has been used to implement braking analysis in this thesis work. The command speed is assumed to be the primary command from which all other command signals are generated.

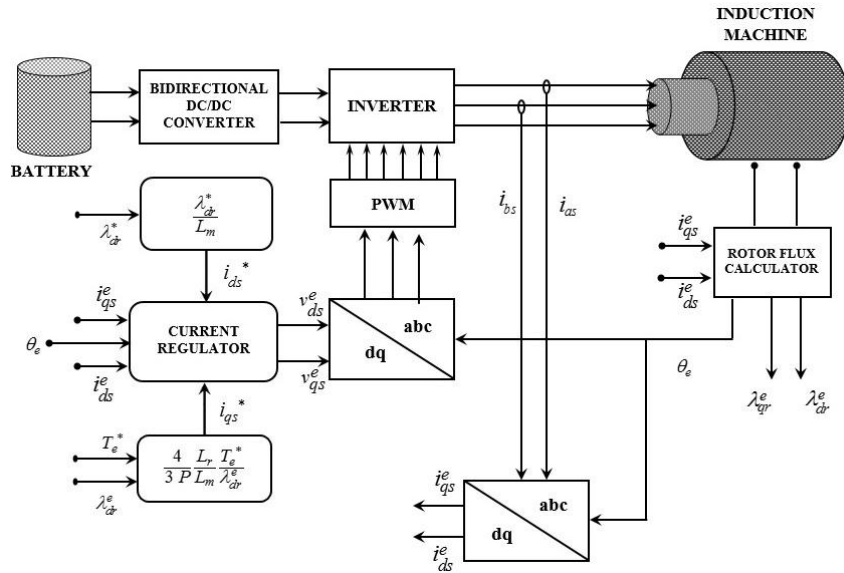


Fig. 3.9. Field oriented control of induction machine

The torque command is developed in accordance with the speed command using an anti-windup speed regulation controller. The feedback integration of the anti-windup prevents the integrator from integrating speed error beyond the maximum and minimum values of the torque command stated as depicted in Fig. 3.10. This command torque T_e^* is required for producing the necessary command current in stator q-axis i_{qs}^* as calculated through Eqn. 3.7. The command value of stator current in d-axis i_{ds}^* can be determined from the command value of rotor flux (λ_{dr}^*) from Eqn. 3.8.

$$i_{qs}^* = \frac{4 L_r T_e^*}{3 P L_m \lambda_{dr}^*} \quad (3.7)$$

$$i_{ds}^* = \frac{\lambda_{dr}^*}{L_m} \quad (3.8)$$

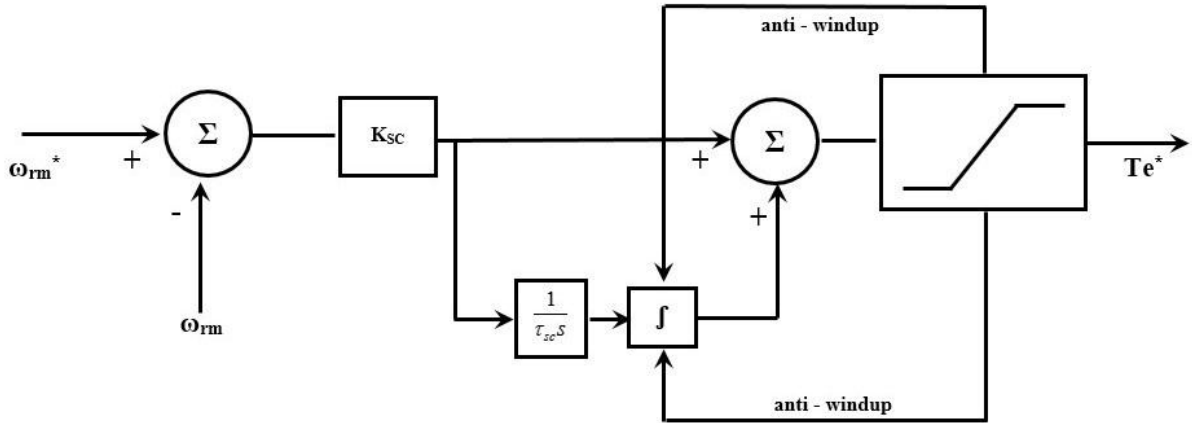


Fig. 3.10. Speed and torque control

These command values of currents (i_{qs}^* and i_{ds}^*) are taken as inputs to the current controller that produce the voltage commands i.e. v_{qs}^* and v_{ds}^* as outputs. These current commands are regulated with the actual values of current in q-axis (i_{qs}^e) and d-axis (i_{ds}^e) so as to develop the required voltage commands through the voltage based current regulator as discussed in the next section. The command voltages of stator q-axis (v_{qs}^*) and d-axis (v_{ds}^*) in the synchronously reference frame are transformed to 3 Φ system using inverse transformation which are used to trigger the inverter.

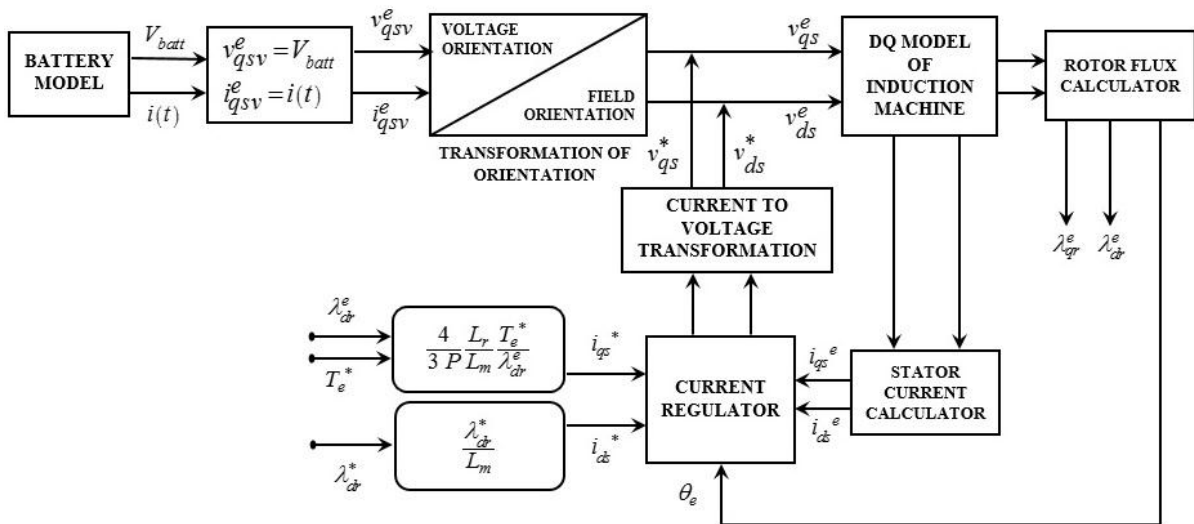


Fig. 3.11. Field oriented control of induction machine model

The inverter is connected to the battery through a bidirectional converter as shown in Fig. 3.9. The 3 Φ voltages from the inverter drives the motor maintaining the required command

speed. Although this is the method for practical implementation of FOC, inverter and bi-directional converter circuits can be bypassed by carrying out the entire analysis in the synchronously rotating frame. This completely focusses on the performance of the traction drive and reduces the complexity. The implementation of FOC using the dynamic model of induction machine and the battery model has been shown in Fig. 3.11. The regenerative braking analysis has been simulated in accordance with this block diagram.

The complexity of the analysis has been simplified by using the dynamic model of the IM. For the dynamic model of IM, the entire analysis of determining command voltages of stator q-axis (v_{qs}^*) and d-axis (v_{ds}^*) is similar to that of 3Φ system as already discussed. As the inverter circuit has been bypassed, the command values of voltages are directly taken as input voltage for the dynamic model of IM. The stator input voltages in both q-axis and d-axis are made non zero through suitable orientation of the rotor flux and current vectors. This complicates the connection of the battery model with the machine model. Hence a mathematical transformation from voltage orientation to field orientation and vice versa is performed to establish a proper mathematical relationship between the battery model and the dynamic model of induction motor. Thus the battery model can be mathematically connected to the machine model through the equations $v_{qs} = V_{\text{batt}}$, and $i_{qs} = i(t)$.

3.3.2 Voltage Source Based Current Control

The realisation of the stator currents fed to a 3Φ machine are analysed through the use of current regulated PWM inverters (CRPWM). The two main types of CRPWM inverters include hysteresis regulator and sine triangle comparison regulator. The hysteresis regulator is quite difficult to model as it is highly nonlinear in nature. However, the sine triangle regulator is basically a linear controller which implements natural sampling PWM algorithm with PI compensation. The sine triangle regulator generally works with operating frequency in the stationary reference frame and hence it is often called as the stationary regulator. However an analysis of this regulator shows that the stationary regulator has an inherent characteristic of degradation of steady state current. The steady state as well as the transient performance is also dependent on load, machine impedance and operating frequency. Hence in [42, 44] a synchronous regulator has been proposed which regulates the ac currents without phase lead compensation. The steady state error of synchronous regulator is zero and the transient performance is more independent of load, motor impedance and operating frequency in

comparison to the stationary regulator. It also does not increase the complexity of circuit significantly.

Synchronous regulator can be designed with an integral feedback loop where either a voltage modulation strategy is used to obtain voltage source command or a current modulation strategy is used to obtain current source command [12]. In this analysis a voltage source based current control has been implemented as shown in Fig. 3.12, where a voltage modulation strategy is used to obtain current command. The command currents in q-axis (i_{qs}^*) and d-axis (i_{ds}^*), the measured values of actual currents in the q-axis (i_{qs}^e) and d-axis (i_{ds}^e), and the machine speed (ω_e) in the synchronous reference frame are taken as the input to the controller. The command values for the voltages in q-axis (v_{qs}^*) and d-axis (v_{ds}^*) in the synchronous reference frame are the outputs of the controller. The parameters implemented in this control strategy include the regulator gain (K_r), time constant (τ_r), and a Thevenin equivalent inductance of the load (L_T).

The expressions for the command values of the q-axis and d-axis voltages in the synchronous reference frame as obtained from the defined control strategy (Fig. 3.12) are given as

$$v_{qs}^* = (i_{qs}^* - i_{qs}^e) \left[K_r \left(1 + \frac{1}{\tau_r s} \right) \right] - i_{ds}^e L_T \omega_e \quad (3.9)$$

$$v_{ds}^* = (i_{ds}^* - i_{ds}^e) \left[K_r \left(1 + \frac{1}{\tau_r s} \right) \right] - i_{qs}^e L_T \omega_e \quad (3.10)$$

In the analysis with the dynamic model of IM, the inverter has been bypassed, hence to understand the operation of this control loop, the actual measured values of voltages of stator q-axis (v_{qs}) and d-axis (v_{ds}) are assumed to be equal to the respective command voltages of stator q-axis (v_{qs}^*) and d-axis (v_{ds}^*). The actual values of voltages of stator q-axis (v_{qs}) and d-axis (v_{ds}) are calculated in Appendix 4.

$$v_{qs} = v_{qs}^* \quad (3.11)$$

$$\omega_e L_T i_{ds} + p L_T i_{qs} + e_{qT} = (i_{qs}^* - i_{qs}) \left[K_r \left(1 + \frac{1}{\tau_r s} \right) \right] - i_{ds} L_T \omega_e \quad (3.12)$$

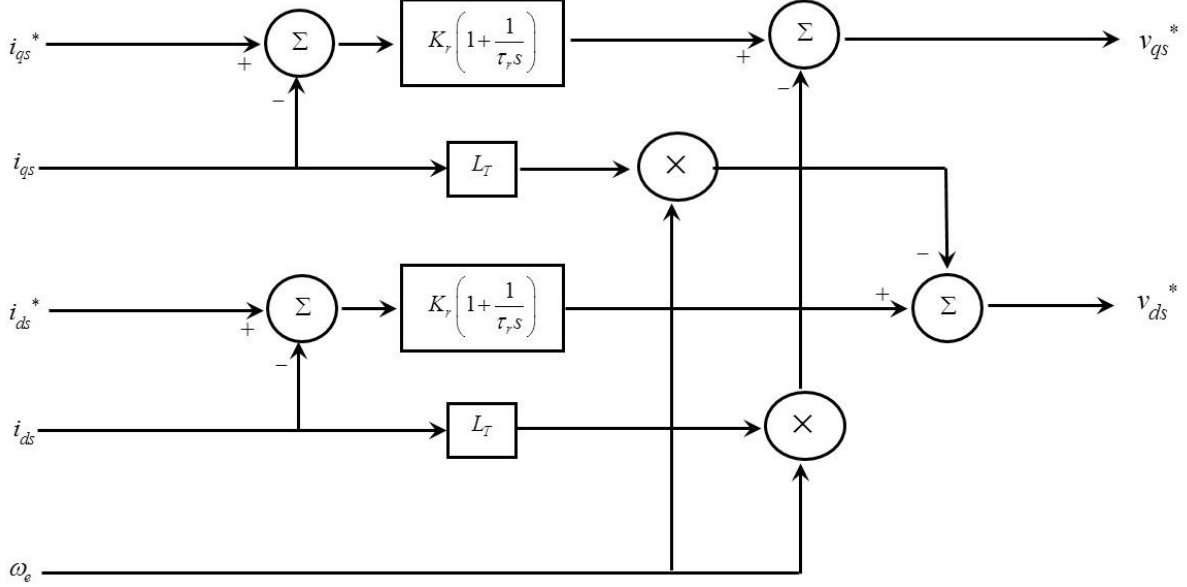


Fig. 3.12. Voltage source based current controller

Solving Eqn. 3.12 for i_{qs} we have

$$i_{qs} = \frac{K_r (\tau_r s + 1) i_{qs}^* + e_{qT} \tau_r s}{\left[p + \frac{K_r}{L_T} \left(1 + \frac{1}{\tau_r s} \right) \right] \times L_T} \quad (3.13)$$

Substituting the derivative term (p) into the Laplace domain (s) and arranging the terms we have

$$i_{qs} = \frac{K_r (\tau_r s + 1) i_{qs}^* + e_{qT} \tau_r s}{L_T \tau_r \left[s^2 + \frac{K_r}{L_T} s + \frac{K_r}{L_T \tau_r} \right]} \quad (3.14)$$

Similarly the expression for the d- axis current i_{ds} can be obtained.

The Eqn. 3.14 shows that there will be no steady state error and there is no interaction between the q- axis and d- axis. This interaction has been eliminated by the Thevenin equivalent

of load inductance (L_T). The pole placement technique can be used to determine the values of the time constant (τ_r) and the regulator gain (K_r). From Eqn. 3.14 the characteristic equation of the designed control algorithm can be obtained as

$$s^2 + \frac{K_r}{L_T} s + \frac{K_r}{L_T \tau_r} = 0 \quad (3.15)$$

Since the given characteristic equation is quadratic in nature, thus it will have two poles i.e. s_1 and s_2 . Applying the laws governing the roots of a quadratic equation we have

$$s_1 + s_2 = \frac{K_r}{L_T} \quad (3.16)$$

$$s_1 \times s_2 = \frac{K_r}{L_T \tau_r} \quad (3.17)$$

Solving Eqn. 3.16 for regulator gain we have

$$K_r = L_T (s_1 + s_2) \quad (3.18)$$

Substituting the value of K_r in Eqn. 3.17, the value of the time constant (τ_r) is obtained as

$$\tau_r = \frac{1}{s_1} + \frac{1}{s_2} \quad (3.19)$$

The generalized expression of the characteristic equation of a transfer function is given as

$$s^2 + 2\zeta\omega_n s + \omega_n^2 = 0 \quad (3.20)$$

where ζ gives the damping ratio and ω_n gives the natural frequency of the signal. In this case the characteristic equation for the transfer function of the designed control algorithm is given by Eqn. 3.15. Comparing Eqn. 3.15 and Eqn. 3.20, we have

$$2\zeta\omega_n = \frac{K_r}{L_T} \text{ and } \omega_n^2 = \frac{K_r}{L_T \tau_r} \quad (3.21)$$

Considering a critically damped system with the assumption that both the poles are equal

$$s_1 = s_2 \approx \frac{\omega_1}{10} = \frac{\pi f_1}{5} \quad (3.22)$$

where $\frac{1}{f_1}$ is the simulation step time in Matlab. In practical application where an inverter is used, f_1 is replaced with the switching frequency f_{sw} .

Substituting in Eqn. 3.18 and Eqn. 3.19 we have

$$K_r = 2 \times L_T \times s_1 \quad (3.23)$$

$$\tau_r = \frac{2}{s_1} \quad (3.24)$$

3.3.3 Results And Discussion

The vehicle performance with regenerative braking has been analyzed using 3- Φ , 460-V, 50-hp, 60-Hz, 4-pole IM. The machine with parameters listed in Table II of Appendix 2 is simulated with MATLAB software. The load of the traction machine is given in Eqn. 2.18. The machine initially at rest is driven by a command speed ω_c , as shown in Fig. 3.13. The machine accelerates with the speed ω_r and therein at $t = 3$ s, the regenerative braking is initiated. With the regenerative braking process the vehicle retards faster at higher speed, but the rate of retardation decreases at lower speeds. Hence it takes more than 3 s for coming to zero speed as shown in Fig. 3.13. This shows the inefficiency of regenerative braking at lower speeds.

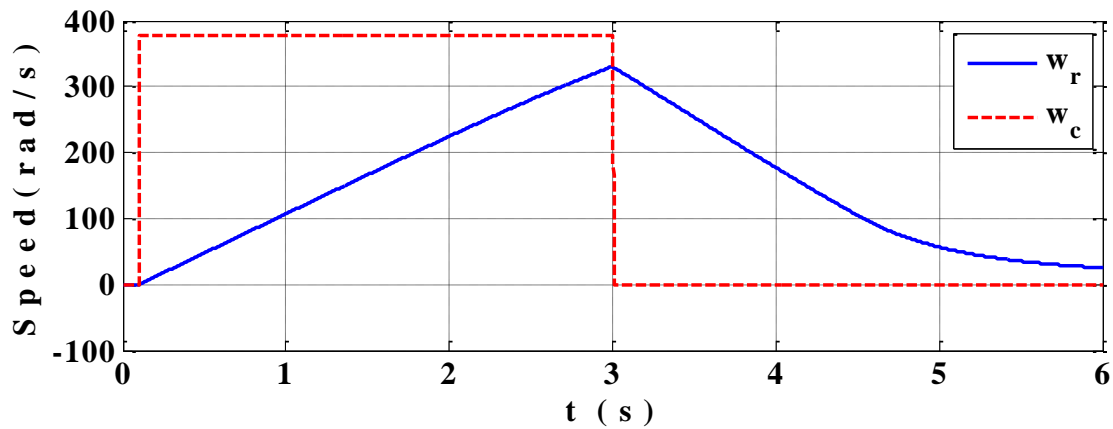


Fig. 3.13. Variation of machine speed with regenerative braking

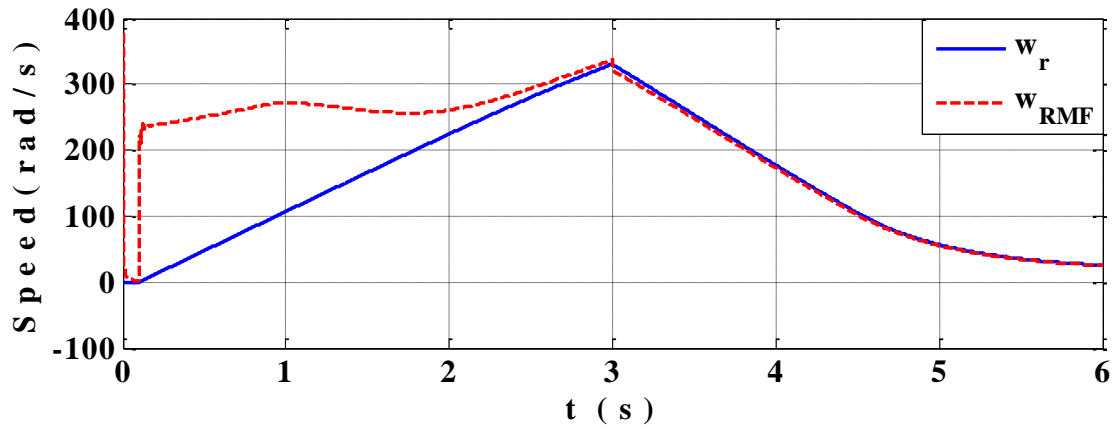


Fig. 3.14. Variation of RMF speed of machine with regenerative braking

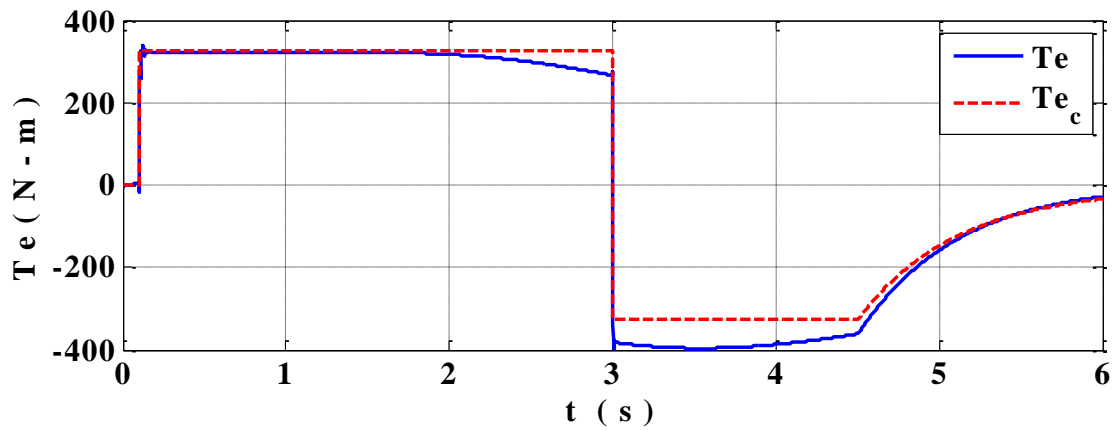


Fig. 3.15. Variation of machine torque with regenerative braking

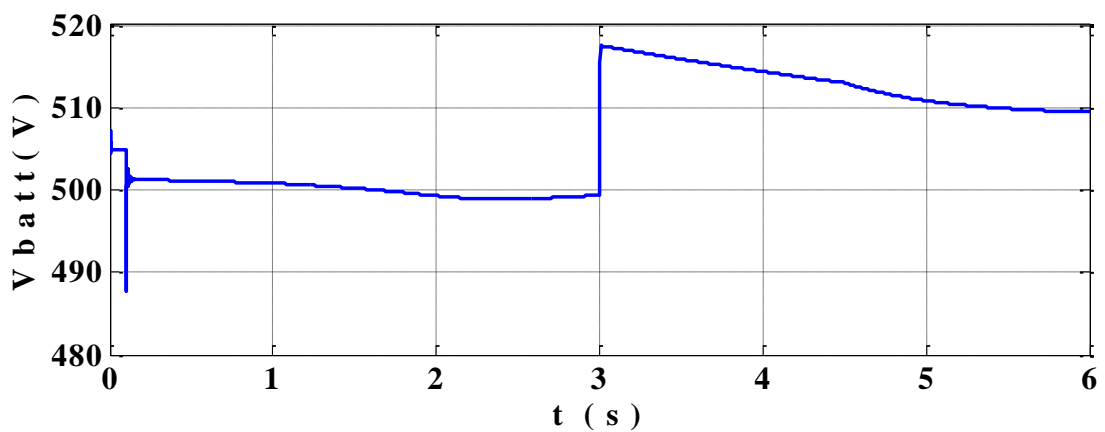


Fig. 3.16. Variation of battery voltage with regenerative braking

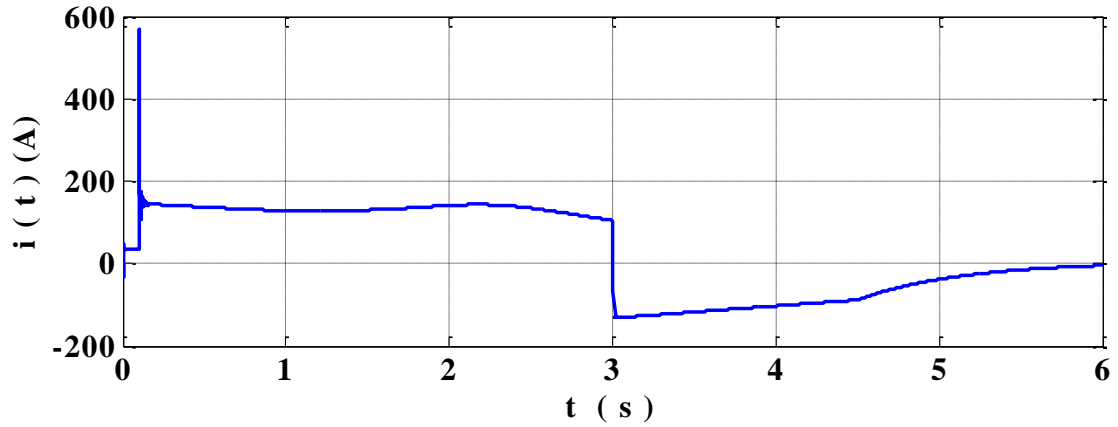


Fig. 3.17. Variation of battery current with regenerative braking

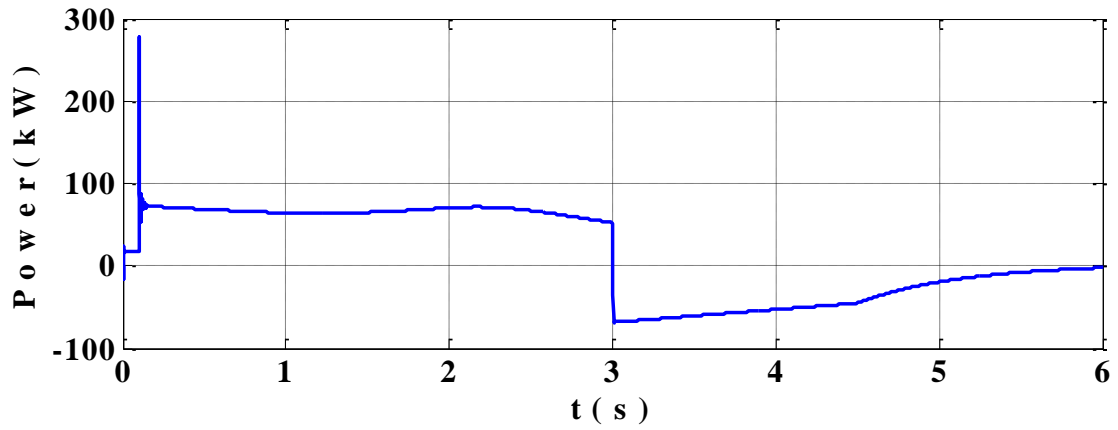


Fig. 3.18. Variation of power with regenerative braking

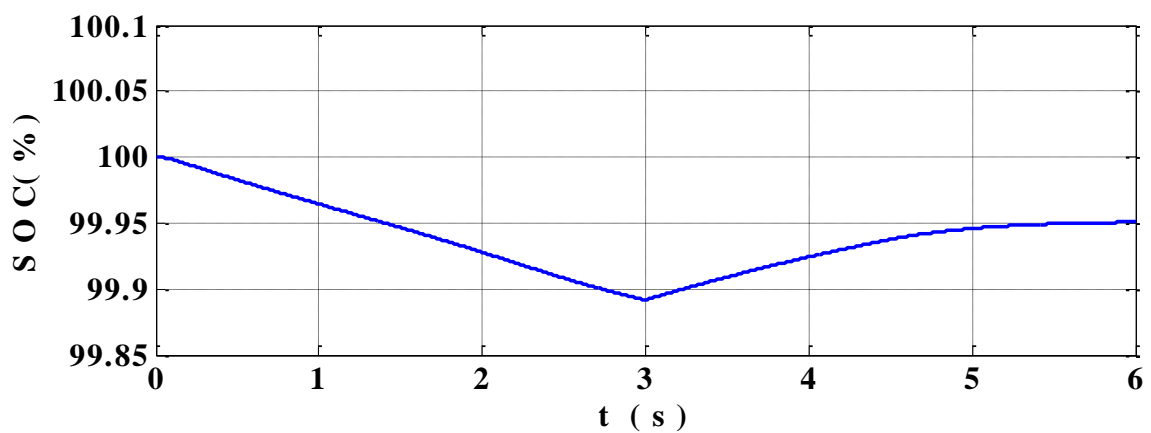


Fig. 3.19. Variation of SOC of battery with regenerative braking

The machine torque during this instant attains a negative value of -380 N-m which can be used as the braking torque as shown in Fig. 3.15. In Fig. 3.16 the battery voltage increases from its normal value and the voltage remains positive throughout. The decrease of the battery current to negative values after braking as shown in Fig. 3.17 indicates that the machine supplies power to the battery during the braking process. After the braking has been initiated, the RMF speed is below the rotor speed as shown in Fig. 3.14 i.e. the machine is operating with a negative slip which indicates regeneration. The power is negative during the braking process which shows the regeneration as shown in Fig. 3.18. The rise in SOC from 99.89 % to 99.95 % during braking (Fig. 3.19) also indicates regeneration.

3.4 SUMMARY

In this chapter, the performance induction machine and battery characteristics both during plug braking and regenerative braking have been analyzed. The auxiliary motor used for plug braking analysis is subjected to voltage oriented control and the main traction motor used for regenerative braking analysis is analyzed with field oriented control. From the results it can be concluded that the plug braking retards the vehicle in a shorter duration in comparison to regenerative braking. The inefficiency of regenerative braking at lower speeds has been clearly outlined. A sufficient amount of power being developed under the effect of regenerative braking is restored back into the battery. Thus, both plug braking and regenerative braking have their own individual advantages. In the next chapter a hybrid electrical braking has been presented, implementing the advantages of both plugging and regenerative braking, which improves the overall braking performance of the vehicle.

CHAPTER 4
BRAKING ANALYSIS BY INTEGRATING PLUG
BRAKING WITH REGENERATIVE BRAKING

INTRODUCTION
HYBRID ELECTRICAL BRAKING SYSTEM
RESULTS AND DISCUSSION
SUMMARY

4.1 INTRODUCTION

In this chapter a hybrid electrical braking system is proposed in which plug braking is integrated with regenerative braking so as to improve the total efficiency of braking both in terms of braking duration and braking energy being regenerated. The regenerative mode of braking is implemented through the main driving motor. An auxiliary motor is used in parallel with the main motor. The plug braking is implemented through the auxiliary motor.

4.2 HYBRID ELECTRICAL BRAKING SYSTEM

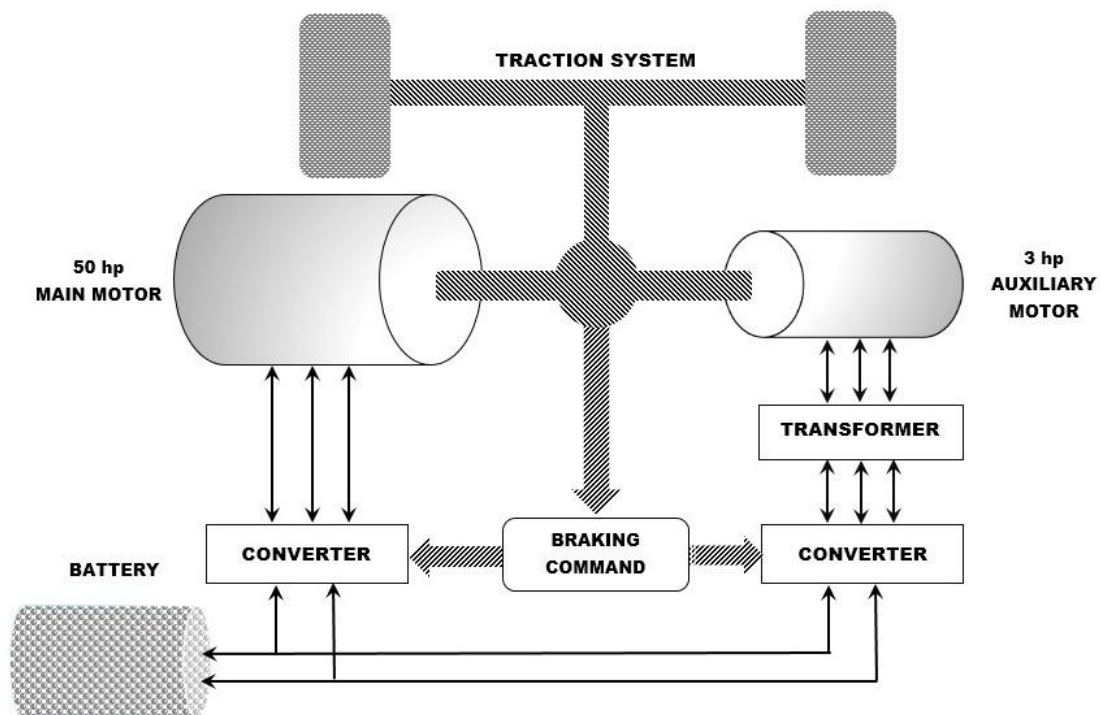


Fig. 4.1. Block diagram of hybrid electrical braking system

In the previous chapter the advantages of both plug braking and regenerative braking have been outlined. However each of the electrical braking method described has its own drawbacks. In order to improve the effectiveness of electrical braking, both regenerative braking and plug braking can be used simultaneously where in the general case of normal braking the former is used, while for requisite cases of fast braking the latter method is used. This can be achieved by using an auxiliary induction motor in parallel to the main traction motor. Both the motors can be used also for the purpose of acceleration when higher speed is

required. The traction system is driven by two induction machines as shown in Fig. 4.1 quite similar to the parallel topology of Electric Vehicle.

One of the induction machine is of rating sufficient enough to drive the vehicle on its own. In this case a 50 hp induction motor (Appendix 2) supplied by 460 V lithium ion battery has been used. During normal operation the main motor is used as the traction drive. This machine is also used to manifest the regenerative braking method whenever normal retardation is required. The auxiliary machine is an induction machine of comparatively lower rating of 3 hp which is supplied by 220 V. An external resistance of around 8Ω is connected to the rotor circuit of the auxiliary motor so as to decrease the peak magnitude of the transient current due to plug braking. A transformer along with an inverter is assumed to be used to step down the battery voltage to the required level of supply voltage for the auxiliary motor. This machine doesn't possess the capacity to drive the vehicle on its own and hence it is normally kept in off state. The machine comes into play only when quicker braking is required, usually at low speeds. Plug braking applied to this machine retards the vehicle in a shorter duration. As the machine is normally in a cool state, the rise in thermal energy in the machine during braking hardly affects the machine windings. The vehicle is driven under the combined effect of both motors. The auxiliary motor is energized only with the requirement of faster braking depending on the driver's requirement of braking torque.

Under the braking effect of both the motor, the negative torque produced in either case of plugging and regenerative braking gets added up so as to have comparatively larger braking torque which retards the vehicle faster in a shorter braking duration. The plug braking is non regenerative in nature as discussed in the previous chapter. Hence the positive current produced during plugging reduces the magnitude of negative current due to regenerative braking. Hence the net battery current though remains negative but its magnitude remains within the rated limits of the machine. This analysis has been discussed in the following section. The same analysis can be carried out with 50 Hz supply in order to follow the Indian Standards.

4.3 RESULTS AND DISCUSSION

To study the improvement of vehicle performance with the proposed hybrid electrical braking system, the vehicle with parameters listed in Table. I is simulated in MATLAB using 2 induction machines of rating 3- Φ , 460-V, 50-hp, 60-Hz, 4-pole used as the main traction motor, and 3- Φ , 220-V, 3-hp, 60-Hz, 4-pole IM used as auxiliary motor whose parameters are listed in Table. II and Table. III respectively in Appendix 2.

The machine is driven by a vehicle load given in Eqn. 2.18. The variation of vehicle speed is shown in Fig. 4.2. Initially the vehicle is at rest at $t = 0$ s. The machine is then driven through a typical command speed ω_c accelerating to $t = 3$ s. The vehicle accelerates with a speed ω_r due to the electromagnetic torque produced by the main motor only. When a slightly more torque is required during cruising or hill climbing, the additional torque can be provided by the auxiliary motor by connecting it to the supply in the same phase sequence as that of the main motor.

For application of braking mode in the vehicle, the main motor undergoes regenerative braking mode and the auxiliary motor undergoes plug braking mode simultaneously. A comparative study has been made between hybrid braking and regenerative braking by analysing the performance of the main motor and the battery parameters. When the brake is applied at $t = 3$ s, the vehicle speed gradually retards and finally becomes zero at $t = 5$ s. As shown in Fig. 4.2, the braking performance of the vehicle with the hybrid braking has a significant improvement in vehicle duration in comparison to regenerative braking used alone. Here the rate of retardation with the application of the hybrid brakes has consistently increased. The regenerative braking at low speed has been superimposed by plugging to attain a better retardation. Fig. 4.3 shows that during hybrid braking, a negative torque is produced which is used as the braking torque to bring the necessary retardation. The braking torque has a peak magnitude of -550 N-m due to the added effect of braking torque due to plugging of auxiliary motor, in contrast to braking torque of -380 N-m produced by regenerative braking alone. The increased braking torque brings in faster retardation.

The battery voltage increases to 518 V at the instant of braking using hybrid braking as shown in Fig. 4.4. The main motor used for regenerative braking produces a peak current of -135 A. Such a high value of peak current has been reduced to -60 A with hybrid braking due to the effect of positive currents produced by the plug braking of auxiliary motor as shown in Fig. 4.5. But since the net battery current during braking is negative, there is regeneration of power into the battery as shown in Fig. 4.6. The power being regenerated is about -50 kW with hybrid braking, which is comparatively less than with regenerative braking. This is because of the power consumed by the auxiliary machine under the effect of plugging. The regeneration of power into the battery increases the SOC of the battery from 99.89% to 99.92% after braking as shown in Fig. 4.7.

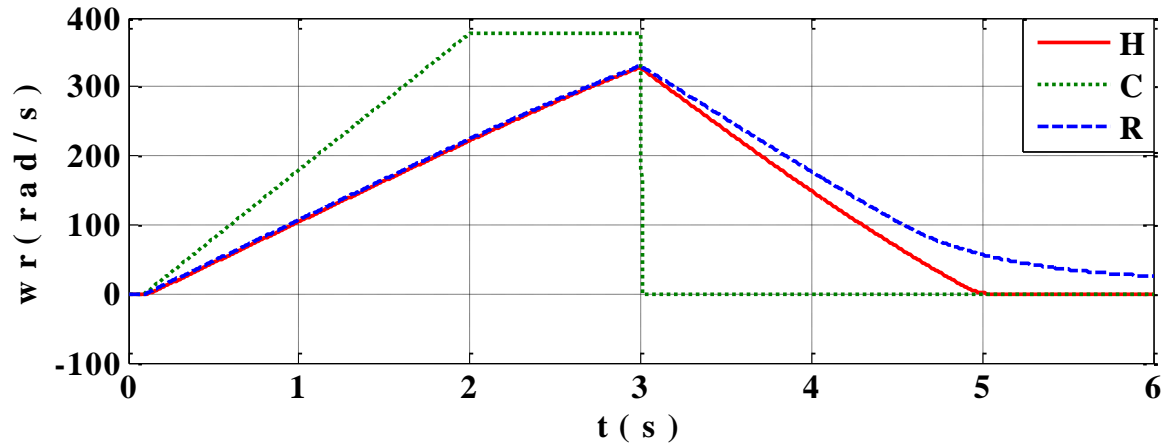


Fig. 4.2. Variation of vehicle speed with hybrid braking system

H: Hybrid Braking; R: Regenerative Braking; C: Command Value

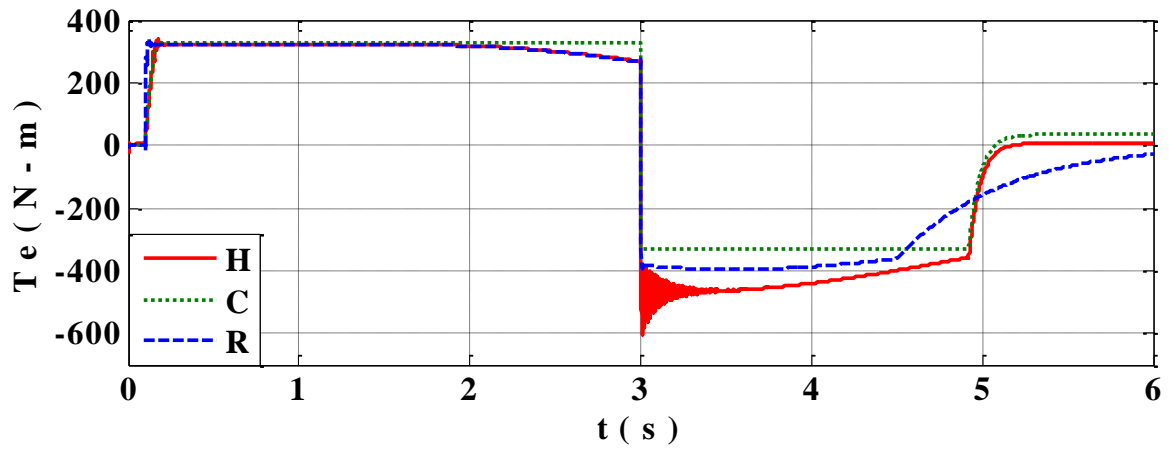


Fig. 4.3. Variation of torque with hybrid braking system

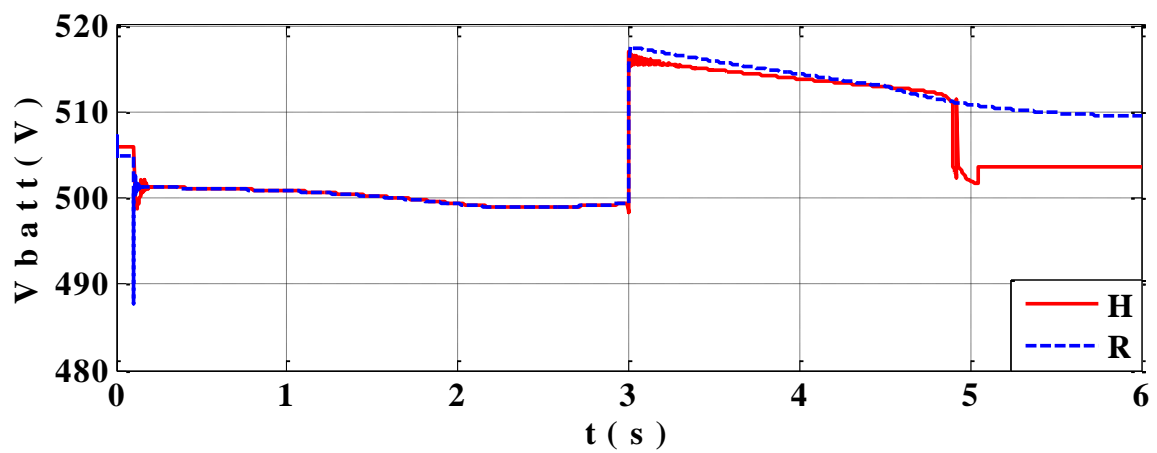


Fig. 4.4. Variation of battery voltage with hybrid braking system

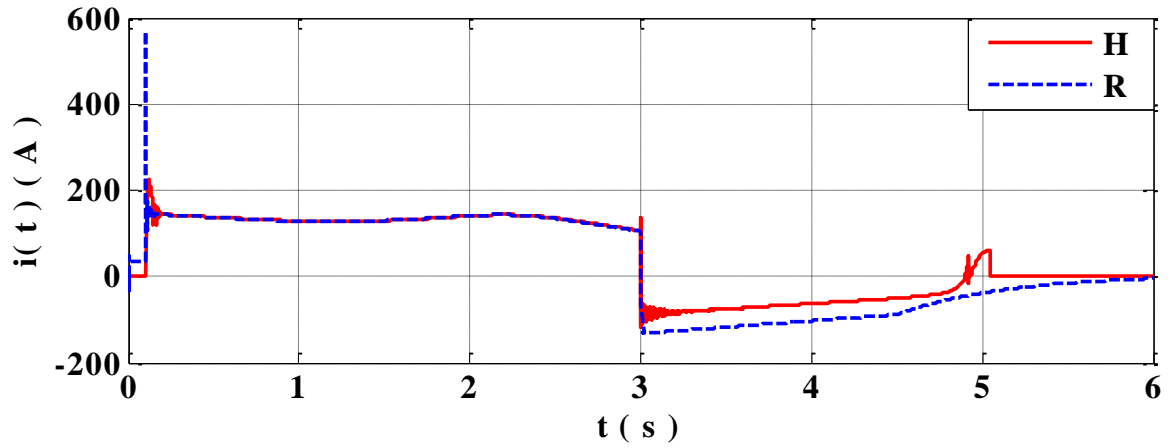


Fig. 4.5. Variation of battery current with hybrid braking system

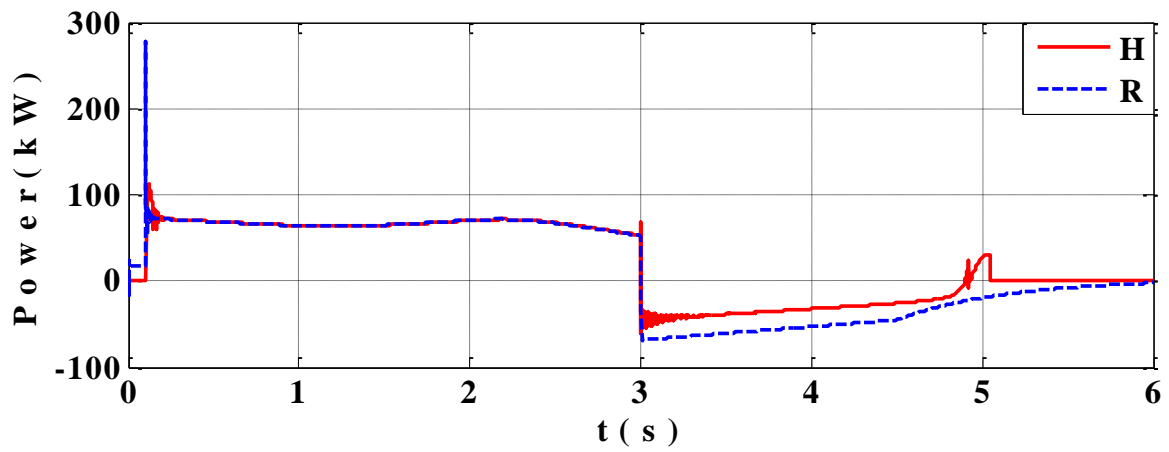


Fig. 4.6. Variation of power with hybrid braking system

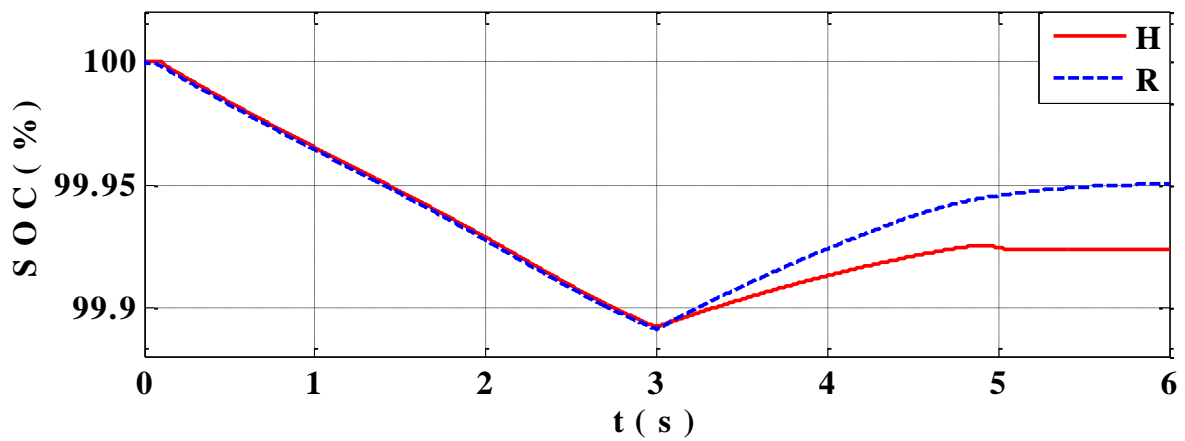


Fig.4.7. Variation of SOC of battery with hybrid braking system

In comparison to regenerative braking used alone, the percentage change in SOC after braking has been reduced with hybrid braking. However, this depends on the intensity of braking (commanded deceleration). For low deceleration command, more energy is regenerated and less energy is used in plugging. In this case controlled plugging can be used by operating the auxiliary motor at reduced speed by keeping V/f constant (operating flux constant).

At low speeds the regenerative braking becomes ineffective, hence plug braking brings about the final retardation. Hence there is a sudden dip in the battery voltage (Fig. 4.4) along with a rise in the current (Fig. 4.5) and machine power (Fig. 4.6) at $t = 5$ s. When the speed of the vehicle is nearly zero the supply to the machine is cut off and a mechanical device is assumed to be used such that it restricts the vehicle to travel in reverse direction.

4.4 SUMMARY

The hybrid electrical braking system proposed in this chapter governs the braking process of the vehicle more effectively. This improved braking system combines the advantages of both regenerative braking and plug braking. The braking duration is reduced in comparison to the normal method of regenerative braking. However, this method regenerates a substantial amount of energy being wasted during the braking process like the regenerative braking method in contrast to the plug braking method. The high values of negative current of the main motor during the instant of braking are compensated to lower values under the effect of positive currents produced by the auxiliary motor with plug braking. Hence the overall braking performance of the machine and battery used for driving the vehicle have been improved.

CHAPTER 5
CONCLUSION AND SCOPE FOR FUTURE WORK

CONCLUSION
SCOPE FOR FUTURE WORK

5.1 CONCLUSION

The use of auxiliary motor along with main motor shows similar braking performance as that of mechanical braking used along with main motor. If mechanical braking system is to act when battery currents exceed tolerable values, a servo control mechanism with a sensor may be necessary to control hydraulic braking, which is more complex and costly.

In the proposed method of hybrid electric braking, desired braking is obtained keeping the battery currents in limits. The hybrid braking improves the braking duration by using plug braking simultaneously with regenerative braking. Under the combined effect of both regenerative braking and plug braking, the retardation of the machine is improved and the braking duration is decreased. The auxiliary motor and the main motor also have electrical interaction unlike the present hybrid mechanical braking system, through which the magnitude of the negative currents produced by regenerative braking beyond the maximum limits of the machine are reduced in magnitude by the added effect of the positive currents produced by plug braking in the auxiliary motor. The auxiliary motor can also provide accelerating torque whenever required in addition to the torque produced by the main motor but this is not possible in the case of hybrid mechanical braking system.

5.2 SCOPE FOR FUTURE WORK

The work is focused here on battery and induction machines only, so intermediate components necessary for real time implementation are bypassed. A simulation study can be performed with properly designed converters and filters. The use of external resistance for the auxiliary motor can be avoided by a proper design of the rotor of auxiliary motor using Finite Element Analysis (FEA). The rotor of the auxiliary motor can be designed with light weight conductors having high resistance (long conductors with less rotor radius). This arrangement provides less current during plugging and less moment of inertia. Initial experimental study can be carried out in a laboratory with a constant load. Implementing in an actual vehicle and testing its performance gives completeness to this work.

APPENDIX 1

PROTOTYPES OF HEV

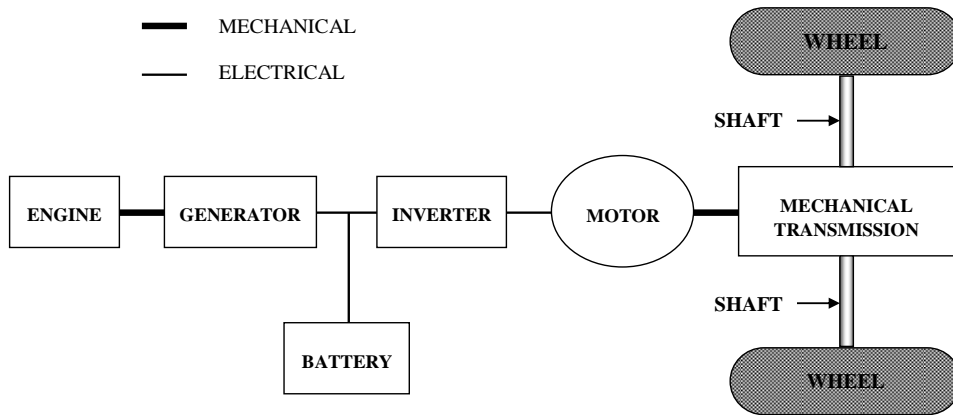


Fig. A1.1. Block diagram of series HEV

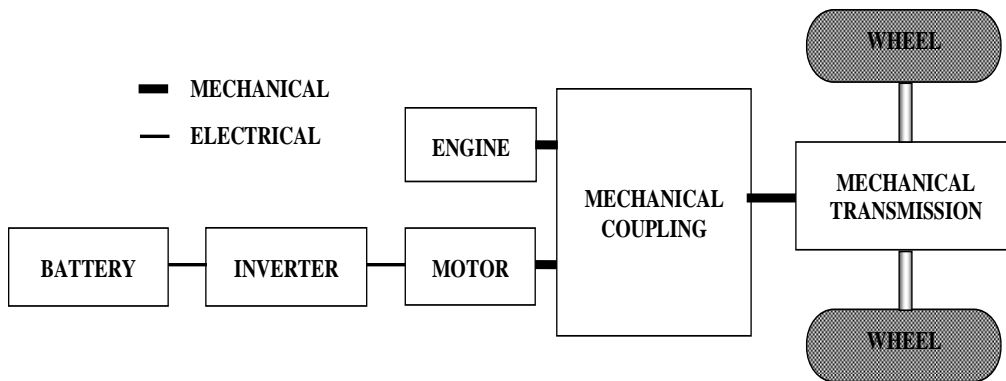


Fig. A1.2. Block diagram of parallel HEV

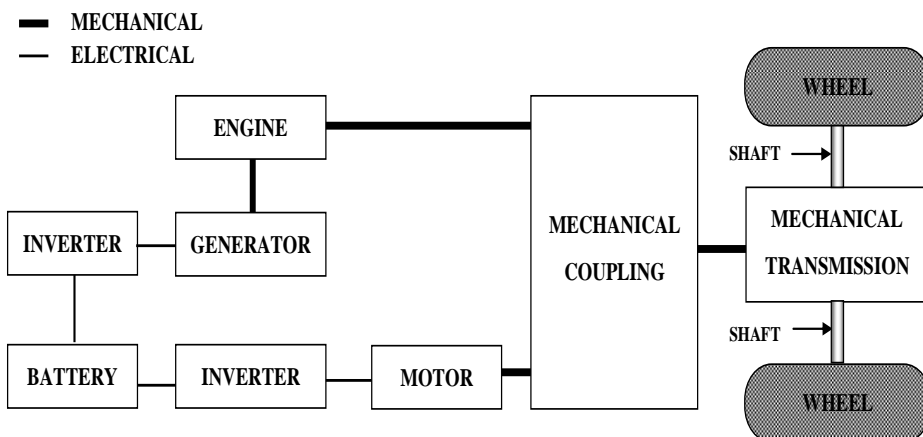
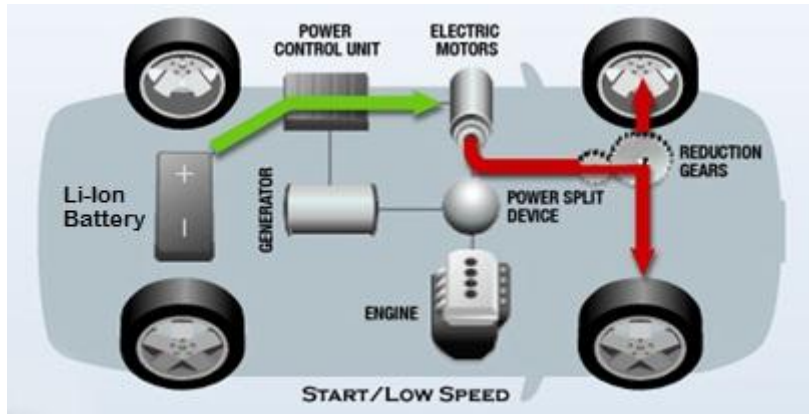
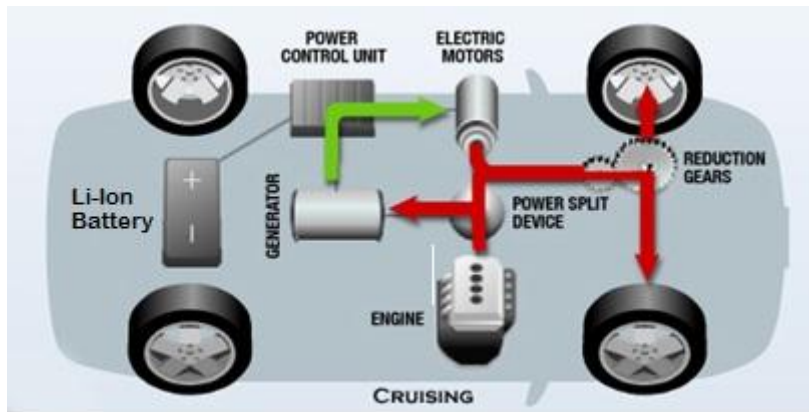


Fig. A1.3. Block diagram of series-parallel HEV



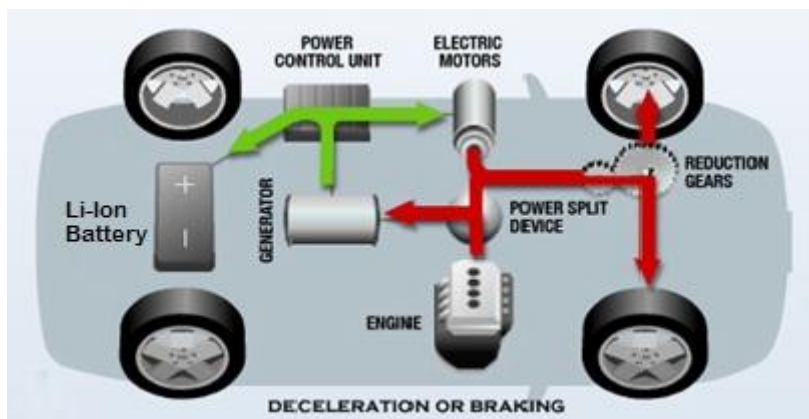
During the starting of the vehicle, the ICE is kept off and the electrical battery drives the vehicle as it can produce high torque in the low speed region

Fig. A1.4. Power flow during starting of the vehicle with Li-Ion battery [43]



During cruising the ICE can be used efficiently to drive the wheels as well as the generator to store power in the battery. The power to the wheels is transferred with minimal loss

Fig. A1.5. Power flow during cruising of the vehicle with Li-Ion battery [43]



The kinetic energy of the vehicle makes the wheels turn the motor through which the energy is regenerated. The frictional energy that is normally wasted as heat is recovered and restored in to the battery to be reused

Fig. A1.6. Power flow during braking of the vehicle with Li-Ion battery [43]

APPENDIX 2

PARAMETERS OF VEHICLE AND INDUCTION MACHINES USED

TABLE I VEHICLE PARAMETERS

SL. NO	PARAMETERS	SYMBOLS	VALUES
1	Curb Weight	m_v	1313 Kg
2	Drag Coefficient	C_d	0.3
3	Frontal Area	A_f	1.746 m ²
4	Rolling Resistance	f_r	0.009
5	Tire Radius	r_w	0.29 m
6	Gear Ratio	g_{dr}	4.1
7	Drive Line Efficiency	n_{dr}	0.95
8	Road Slip	s_x	0.1
9	Friction Coefficient	u_{s0}	3.4
10	Max Power	P_m	50 kW
11	Max Torque	T_m	400 N-m

TABLE II MACHINE PARAMETERS OF 50-HP INDUCTION MOTOR

SL. NO.	PARAMETER	REPRESENTATION	VALUE
1	Voltage	V_{RMS}	460 V(1-1 rms)
2	Poles	P	4
3	Stator Resistance	R_s	0.725 Ω
4	Rotor Resistance	R_r	0.413 Ω
5	Stator Leakage Reactance	X_{ls}	0.497 Ω
6	Rotor Leakage Reactance	X_{lr}	0.497 Ω
7	Magnetizing Reactance	X_m	11.34 Ω
8	Base Frequency	f_b	60 Hz
9	Base Torque	T_b	198 N-m
10	Base Current	$I_b(abc)$	46.8 Amps

TABLE III MACHINE PARAMETERS OF 3-HP INDUCTION MOTOR

SL. NO.	PARAMETER	REPRESENTATION	VALUE
1	Voltage	V_{RMS}	220 V(l-l rms)
2	Poles	P	4
3	Stator Resistance	R_s	0.435 Ω
4	Rotor Resistance	R_r	0.816 Ω
5	Stator Leakage Reactance	X_{ls}	0.754 Ω
6	Rotor Leakage Reactance	X_{lr}	0.754 Ω
7	Magnetizing Reactance	X_m	26.13 Ω
8	Base Frequency	f_b	60 Hz
9	Base Torque	T_b	11.9 N-m
10	Base Current	I_b (abc)	5.8 Amps

APPENDIX 3

CALCULATION OF BATTERY PARAMETERS

The mathematical relationships that can be used to calculate the battery parameters like Battery Constant Voltage (E_0), Internal Resistance (R), Polarization Constant (K), Exponential Zone Amplitude (A), and Exponential Zone Time Constant Inverse (B) from the given ratings of Battery Voltage (V_{batt}) and Battery Capacity (Q) for the required voltages are given by Eqn. A3.1 to Eqn. A3.5. Here subscript (1) indicates the parameters for 3.3 V, 2.3 Ah Li-Ion Battery in [20] and subscript (2) indicates the parameters for 460 V, 100 Ah Li-Ion battery and 220V, 6.5 Ah Li-Ion battery as required by the main motor and auxiliary motor respectively.

$$E_{0(2)} = E_{0(1)} \times \frac{V_{\text{batt}(2)}}{V_{\text{batt}(1)}} \quad (\text{A3.1})$$

$$R_{(2)} = R_{(1)} \times \frac{V_{\text{batt}(2)}}{V_{\text{batt}(1)}} \times \frac{Q_{(1)}}{Q_{(2)}} \quad (\text{A3.2})$$

$$K_{(2)} = K_{(1)} \times \frac{V_{\text{batt}(2)}}{V_{\text{batt}(1)}} \times \frac{Q_{(1)}}{Q_{(2)}} \quad (\text{A3.3})$$

$$A_{(2)} = A_{(1)} \times \frac{V_{\text{batt}(2)}}{V_{\text{batt}(1)}} \quad (\text{A3.4})$$

$$B_{(2)} = B_{(1)} \times \frac{Q_{(1)}}{Q_{(2)}} \quad (\text{A3.5})$$

The main traction motor of rating 3- Φ , 460-V, 50-hp, 60-Hz and 4-pole is used to drive the vehicle under the normal conditions. The battery connected to this machine should be able to drive the vehicle efficiently over a time span in which a nominal distance is covered. Hence the discharge capacity of the battery is determined as 100 Ah.

$$E_0 = 469.20 \text{ V}$$

$$R = 0.0321 \text{ } \Omega$$

$$K = 0.0244 \text{ V/(Ah)}$$

$$A = 36.831 \text{ V}$$

$$B = 0.61062 \text{ (Ah)}^{-1}$$

The auxiliary machine of rating 3- Φ , 220-V, 3-hp, 60-Hz, and 4-pole is interfaced with a battery supplying a rated voltage of 220 V. As this machine comes into use only for shorter duration of time, the rated capacity is taken as 6.5 Ah.

$$\begin{aligned} E_o &= 224.40 \text{ V} \\ R &= 0.2359 \text{ } \Omega \\ K &= 0.1793 \text{ V/(Ah)} \\ A &= 17.614 \text{ V} \\ B &= 9.3941 \text{ (Ah)}^{-1} \end{aligned}$$

APPENDIX 4

CALCULATIONS FOR

VOLTAGE SOURCE BASED CURRENT CONTROL

The stator voltage equations for an induction machine in any arbitrary reference frame are written as

$$v_{qs} = r_s i_{qs} + \omega_e \lambda_{ds} + p \lambda_{qs} \quad (\text{A4.1})$$

$$v_{ds} = r_s i_{ds} - \omega_e \lambda_{qs} + p \lambda_{ds} \quad (\text{A4.2})$$

The flux linkages in the stator and the rotor reference frames are given as

$$\lambda_{qs} = L_s i_{qs} + L_m i_{qr} \quad (\text{A4.3})$$

$$\lambda_{ds} = L_s i_{ds} + L_m i_{dr} \quad (\text{A4.4})$$

$$\lambda_{qr} = L_r i_{qr} + L_m i_{qs} \quad (\text{A4.5})$$

$$\lambda_{dr} = L_r i_{dr} + L_m i_{ds} \quad (\text{A4.6})$$

Neglecting the stator resistance and assuming the rotor flux linkages in the synchronous reference frames to be constant, we have

$$r_s = 0 \quad (\text{A4.7})$$

$$p \lambda_{qr} = \frac{d}{dt} \lambda_{qr} = 0 \quad (\text{A4.8})$$

$$p \lambda_{dr} = \frac{d}{dt} \lambda_{dr} = 0 \quad (\text{A4.9})$$

From Eqn. A4.5 and A4.6 we have

$$i_{qr} = \frac{\lambda_{qr} - L_m i_{qs}}{L_r} \quad (\text{A4.10})$$

$$i_{dr} = \frac{\lambda_{dr} - L_m i_{ds}}{L_r} \quad (\text{A4.11})$$

Starting with Eqn. A4.1

$$v_{qs} = r_s i_{qs} + \omega_e \lambda_{ds} + p \lambda_{qs} \quad (\text{A4.12})$$

Considering the assumptions made in Eqn. A4.7 to Eqn. A4.9 we have

$$v_{qs} = \omega_e \lambda_{ds} + p \lambda_{qs} \quad (\text{A4.13})$$

Substituting the values from Eqn. A4.3 and Eqn. A4.4

$$v_{qs} = \omega_e [L_s i_{ds} + L_m i_{dr}] + p [L_s i_{qs} + L_m i_{qr}] \quad (\text{A4.14})$$

Substituting the values from Eqn. A4.10 and Eqn. A4.11

$$v_{qs} = \omega_e \left[L_s i_{ds} + L_m \left(\frac{\lambda_{dr} - L_m i_{ds}}{L_r} \right) \right] + p \left[L_s i_{qs} + L_m \left(\frac{\lambda_{qr} - L_m i_{qs}}{L_r} \right) \right] \quad (\text{A4.15})$$

Solving the expression mathematically we obtain

$$v_{qs} = \omega_e \left(\frac{L_s L_r - L_m^2}{L_r} \right) i_{ds} + p \left(\frac{L_s L_r - L_m^2}{L_r} \right) i_{qs} + \frac{L_m}{L_r} (\omega_e \lambda_{dr} + p \lambda_{qr}) \quad (\text{A4.16})$$

Substituting

$$\frac{L_m}{L_r} (\omega_e \lambda_{dr} + p \lambda_{qr}) = e_{qT} \quad (\text{A4.17})$$

$$\left(\frac{L_s L_r - L_m^2}{L_r} \right) = L_T \quad (\text{A4.18})$$

The equation for the stator voltage equation of the q- axis can be given as

$$v_{qs} = \omega_e L_T i_{ds} + p L_T i_{qs} + e_{qT} \quad (\text{A4.19})$$

Similarly the stator voltage equation for the d- axis can be given as

$$v_{ds} = -\omega_e L_T i_{qs} + p L_T i_{ds} + e_{dT} \quad (\text{A4.20})$$

where

$$\frac{L_m}{L_r} (\omega_e \lambda_{qr} + p \lambda_{dr}) = e_{dT} \quad (\text{A4.21})$$

e_{qr} , e_{dr} = slowly varying quantities since flux linkages λ_{qr} , λ_{dr} are assumed to be constant

L_T = Thevenin equivalent of the inductance of the load

From Eqn. A4.18, the value of L_T can be approximated as

$$L_T = \left(\frac{(L_m + l_{ls})(L_m + l_{lr}) - L_m^2}{(L_m + l_{lr})} \right) \quad (\text{A4.22})$$

Neglecting the product term ($l_{ls} \times l_{lr}$) in the numerator and neglecting l_{lr} with respect to L_m in the denominator, we have

$$L_T = (l_{ls} + l_{lr}) \quad (\text{A4.23})$$

FLOW CHART FOR IMPROVED BRAKING ANALYSIS

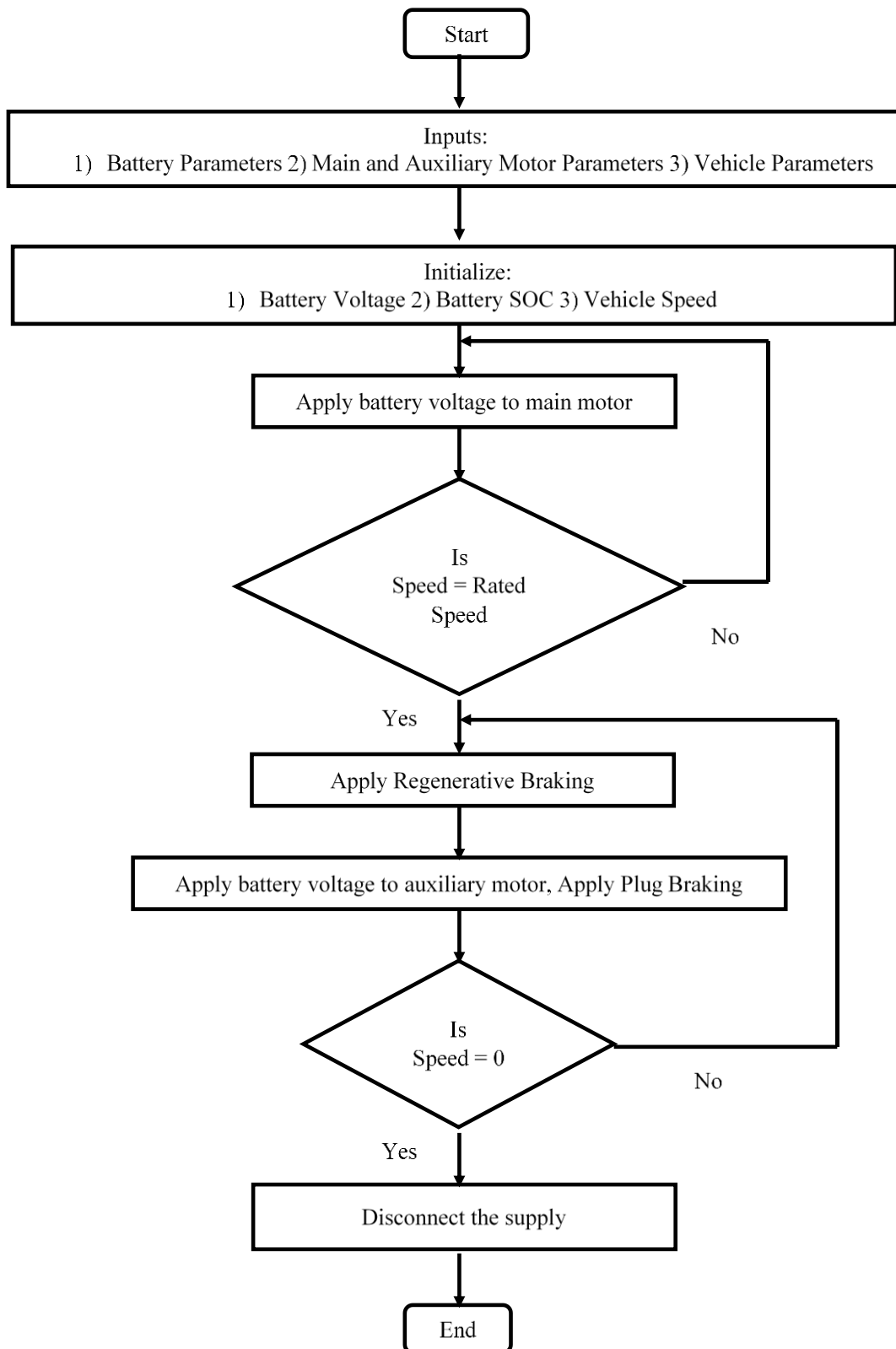


Fig. A5. Flowchart for Simulation Study of Improved Braking Analysis

REFERENCES

- [1] M. Ehsani *et al.*, *Modern Electric, Hybrid Electric, and Fuel Cell Vehicles Fundamentals Theory and Design*. CRC Press, Second Edition, Special Indian Edition, 2007.
- [2] M. Collie, *Electric and Hybrid Vehicles*. Energy Technology Review No. 44, New Jersey, USA, Noyes Data Corporation, 1979.
- [3] C. C. Chan, "The State of Art of Electric Vehicles and Hybrid Vehicles," in *Proc. IEEE*, vol. 90, no. 2, pp. 247-275, Feb. 2002.
- [4] T. M. Jahns, and V. Blasko, "Recent advances in power electronics technology for industrial and traction machine drives," in *Proc. IEEE*, vol. 89, no. 6, pp. 963-975, Jun 2001.
- [5] Chris Mi *et al.*, *Hybrid Electric Vehicles-Principles and Applications with Practical Perspectives*. West Sussex, John Wiley and Sons Pvt. Ltd, 2011.
- [6] Kwang Hee Nam, *AC Motor Control and Electric Vehicle Applications*. CRC Press, Taylor and Francis Group, 2010.
- [7] M. Zeraoulia and M. H. B. Demba Diallo, "Electric Motor Drive Selection Issues For HEV Propulsion Systems: A Comparative Study," *IEEE Trans. Veh. Technol.*, vol. 55, no. 6, pp. 1756-1763, Nov. 2006.
- [8] M. Ehsani *et al.*, "Hybrid Electric Vehicles: Architecture and Motor Drives," in *Proc. IEEE*, vol. 95, no. 4, pp. 719-728, April 2007.
- [9] P. S. Bhimbra, *Electrical Machinery*. Seventh Edition, New Delhi, India, Khanna Publishers, 2011.
- [10] P. S. Bhimbra, *Generalized Theory of Electrical Machines*. Fifth Edition, New Delhi, India, Khanna Publishers, 2009.
- [11] B. K. Bose, *Modern Power Electronics and AC Drives*. New Delhi, India, PHI Learning Private Limited, 2011.
- [12] P. C. Krause *et al.*, *Analysis of Electric Machinery and Drive Systems*. IEEE Press, A John Wiley & Sons, Inc. Publication Second Edition, 2002.
- [13] P. C. Krause and C. H. Thomas, "Simulation of Symmetrical Induction Machinery," *IEEE Trans. Power App. Syst. (until 1985)*, vol. 84, no. 11, pp. 1038-1053, Nov. 1965.
- [14] H. C. Stanley, "An Analysis of the Induction Machine," *Trans. American Institute of Electrical Engineers*, vol. 57, no. 12, pp. 751-757, Dec. 1938.

- [15] B. Ozpineci and L. M. Tolbert, "Simulink implementation of induction machine model - a modular approach," *IEEE International Electric Machines and Drives Conf., IEMDC'03*, vol. 2, pp. 728-734, 1-4 June 2003.
- [16] H.V. Shah, "A modular Simulink implementation of induction machine model & performance in different reference frames," *Int. Conf. Advances in Engineering, Science and Management (ICAESM)*, pp. 203-206, 30-31 March 2012.
- [17] Shuhui Li and Bao Ke, "Study of battery modeling using mathematical and circuit oriented approaches," *IEEE Power and Energy Society General Meeting*, pp. 1-8, 24-29 July 2011.
- [18] H. L. Chan, "A new battery model for use with battery energy storage systems and electric vehicles power systems," in *Proc. 2000 IEEE Power Engineering Society Winter Meeting*, vol. 1, pp. 470-475, 2000.
- [19] O. Tremblay *et al.*, "A Generic Battery Model for the Dynamic Simulation of Hybrid Electric Vehicles," *IEEE Vehicle Power and Propulsion Conf., VPPC*, pp. 284-289, 9-12 Sept. 2007.
- [20] Olivier Tremblay and Louis A. Dessaint, "Experimental Validation of a Battery Dynamic Model for EV Applications," *J. World Electric Vehicle, Vol. 3, EVS24*, Stavanger, Norway, May 13 -16, 2009.
- [21] B. Enache *et al.*, "Comparative study for generic battery models used for electric vehicles," *8th International Symposium on Advanced Topics in Electrical Engineering (ATEE)*, pp. 1-6, 23-25 May 2013.
- [22] Lijun Gao *et al.*, "Dynamic lithium-ion battery model for system simulation," *IEEE Trans. Compon. Packag. Technol.*, vol. 25, no. 3, pp. 495-505, Sep 2002.
- [23] M. L. Kuang *et al.*, "Hydraulic brake system modeling and control for active control of vehicle dynamics," in *Proc. 1999 American Control Conf.*, vol. 6, pp. 4538-4542, 1999.
- [24] S. Anwar *et al.*, "An anti-lock braking control system for a hybrid electromagnetic/electrohydraulic brake-by-wire system," in *Proc. American Control Conf.*, vol. 3, pp. 2699-2704, June 30 2004-July 2 2004.
- [25] M. Covino *et al.*, "Analysis of braking operations in present-day electric drives with asynchronous motors," *IEEE Int. Conf. Rec. Electric Machines and Drives*, pp. MB3/1.1-MB3/1.3, 18-21 May 1997.
- [26] G. Celentano *et al.*, "Regenerative and plug-braking operations of inverter-fed asynchronous motors," *IEE Proc. Electric Power Applications*, vol. 144, no. 6, pp. 453-455, Nov 1997.

- [27] Beck *et al.*, "Plugging an Induction Motor," *IEEE Trans. Industry and General Applications*, vol. IGA-6, no. 1, pp. 10-18, Jan. 1970.
- [28] H. A. Hairik *et al.*, "Proposed scheme for plugging three-phase induction motor," *15th IEEE Mediterranean Electro technical Conf., MELECON*, pp. 1-5, 26-28 April 2010.
- [29] Zhou Lei *et al.*, "A novel brake control strategy for electric vehicles based on slip trial method," *IEEE International Conference on Vehicular Electronics and Safety, ICVES*, pp. 1-6, 13-15 Dec. 2007.
- [30] M. K. Yoong *et al.*, "Studies of regenerative braking in electric vehicle," *Conf. IEEE Sustainable Utilization and Development in Engineering and Technology (STUDENT)*, pp. 40-45, 20-21 Nov. 2010.
- [31] Zechang Sun *et al.*, "Research on Electro-hydraulic Parallel Brake System for Electric Vehicle," *IEEE Int. Conf. Vehicular Electronics and Safety*, pp. 376-379, 13-15 Dec. 2006.
- [32] O. Tur *et al.*, "An Introduction to Regenerative Braking of Electric Vehicles as Anti-Lock Braking System," *IEEE Intelligent Vehicles Symp.*, pp. 944-948, 13-15 June 2007.
- [33] Chen Chih-Keng and Vu Tri-Vein, "Regenerative braking study for a hydraulic hybrid vehicle," *9th World Congress on Intelligent Control and Automation (WCICA)*, pp. 413-418, 21-25 June 2011.
- [34] J. K. Hurtig *et al.*, "Torque regulation with the General Motors ABS VI electric brake system," *Conf. American Control*, vol. 2, pp. 1210-1211, 29 June-1 July 1994.
- [35] M. Kees *et al.*, "Hydraulic actuated brake and electromechanically actuated brake systems," *Int. Conf. Advanced Driver Assistance Systems, (IEE Conf. Publ. No. 483)*, pp. 43-47, 2001.
- [36] Zheng Hongyan and Zhu Tianjun, "Improving Vehicle Stability Using Electro-hydraulic Braking System," *Int. Conf. Information Technology and Computer Science, ITCS*, vol. 1, pp. 593-596, 25-26 July 2009.
- [37] Liang Chu *et al.*, "Integrative control strategy of regenerative and hydraulic braking for hybrid electric car," *IEEE Conf. Vehicle Power and Propulsion, VPPC '09*, pp. 1091-1098, 7-10 Sept. 2009.
- [38] M. Ehsani *et al.*, "Propulsion system design of electric and hybrid vehicles," *IEEE Trans. Ind. Electron.*, vol. 44, no. 1, pp. 19-27, Feb. 1997.
- [39] N. Mutoh *et al.*, "A torque controller suitable for electric vehicles," *IEEE Trans. Ind. Electron.*, vol. 44, no. 1, pp. 54-63, Feb. 1997.

- [40] K. Inoue *et al.*, "A Study on an Optimal Torque for Power Regeneration of an Induction Motor," *Conf. IEEE Power Electronics Specialists*, pp. 2108-2112, 17-21 June 2007.
- [41] S. D. Sudhoff *et al.*, "An induction machine model for predicting inverter-machine interaction," *IEEE Trans. Energy Convers.*, vol. 17, no. 2, pp. 203-210, Jun 2002.
- [42] O. Wasynczuk *et al.*, "A voltage control strategy for current-regulated PWM inverters," *IEEE Trans. Power Electron.*, vol. 11, no. 1, pp. 7-15, Jan. 1996.
- [43] *2014 Global Greenhouse Warming*. [Online]. Available: <http://www.global-greenhouse-warming.com/hybrid-electric-vehicle.html>.
- [44] T. M. Rowan and R. J. Kerkman, "A New Synchronous Current Regulator and an Analysis of Current-Regulated PWM Inverters," *IEEE Trans. Industry Applications*, vol. IA-22, no. 4, pp. 678- 690, July 1986.
- [45] A. B. Nanda and T. K. Bhattacharya, "Stator flux based speed sensor less control of single phase induction motor drives," *Int. Conf. Energy, Automation, Signal (ICEAS)*, pp.1-6, 28-30 Dec. 2011.
- [46] A. B. Nanda and T. K. Bhattacharya, "High performance vector control of single phase induction motor drives based on rotor MEMF," *Int. Conf. Energy, Automation, Signal (ICEAS)*, pp. 1-5, 28-30 Dec. 2011.
- [47] A. Emadi, Lee Joo Young and K. Rajashekara, "Power Electronics and Motor Drives in Electric, Hybrid Electric, and Plug-In Hybrid Electric Vehicles," *IEEE Transactions on Industrial Electronics*, vol.55, no. 6, pp.2237- 2245, June 2008.
- [48] I. Boldea *et al.*, "Automotive Electric Propulsion Systems with Reduced or No Permanent Magnets: An Overview," *IEEE Transactions on Industrial Electronics*, vol. 61, no. 10, pp. 5696 - 5711, Oct. 2014.

THESIS DISSEMINATION

A. A. Mahapatra and S. Gopalakrishna, "Regenerative braking in induction motor drives in applications to Electric Vehicles," *IEEE Students' Conference on Electrical, Electronics and Computer Science (SCEECS)*, pp.1,5, 1-2 March 2014.

doi: 10.1109/SCEECS.2014.6804425

BIO-SKETCH

NAME Amrit Anand Mahapatra

FATHER NAME Aditya Kumar Mahapatra

MOTHER NAME Anulata Mahapatra

DATE OF BIRTH 7th September 1989

EDUCATIONAL DETAIL

MATRICULATION
S. D. P. S. Vidyapeeth, Bhadrak.

INTERMEDIATE
D. A. V Public School, Chandrasekharpur, Bhubaneswar.

GRADUATION
B.Tech (Electrical Engineering), G.H.I.T.M, Puri.

POST GRADUATION
M.Tech-Research (Electrical Engineering),
N.I.T. Rourkela

PRESENT ADDRESS Amrit Anand Mahapatra
Roll No. 611ee105
M.Tech Research
Department of Electrical Engineering
NIT Rourkela
Rourkela, Sundergarh
Odisha, 769008

PERMANENT ADDRESS Amrit Anand Mahapatra
C/O Aditya Kumar Mahapatra
Parents Temple
Canal Road
Charampa, Bhadrak
Odisha, 756101
Tel. No. 06784 230185

EMAIL ID amrit.mahapatra@gmail.com

MOBILE NUMBER 09439492261/09853525588